Annales Societatis Geologorum Poloniae (1993), vol. 63: 33 - 84
PL ISSN 0208-9068

LITHOFACIES AND SEDIMENTATION OF THE BADENIAN (MIDDLE MIOCENE) GYPSUM IN THE NORTHERN PART OF THE CARPATHIAN FOREDEEP, SOUTHERN POLAND

Alicja Kasprzyk

Państwowy Instytut Geologiczny, Oddział Świętokrzyski,
ul. Zgody 21, 25-953 Kielce

Kasprzyk, A., 1993. Lithofacies and sedimentation of the Badenian (Middle Miocene) gypsum in the northern part of the Carpathians Foredeep, southern Poland. *Ann. Soc. Geol. Polon.*, 63: 33 – 84.

A b s t r a c t: The Badenian sulphate sediments are represented by primary gypsum (crystalline selenitic gypsum, massive gypsum, and clastic gypsum), secondary gypsum and anhydrite. Great variety of lithofacies and sedimentary structures is characteristic of the primary gypsum. The studied sediments were laid down in changing conditions – from subaqueous (deep-water to shallow-water) to subaerial, in salinas, and in sabkhas on a gently inclined (< 1°) evaporite ramp of distinct relief. The sequence of lithofacies – *a* through *r* – distinguished in the gypsum sections, is indicative of a general regression, and it includes 6 sedimentary cycles.

Manuscript received 11 March 1991, revised accepted 28 October 1993

INTRODUCTION

Studies on modern evaporite environments enhanced the interpretation of depositional and diagenetic processes in ancient sulphate sediments such as the Messinian sediments of the Mediterranean area (Dronkert, 1985; Schreiber, 1986, 1988; Warren, 1991 and references therein). These sediments – whose interpretation remained controversial for many years (see Warren, 1989) – represent very variable sedimentary environments, from deep-water to subaerial (e.g. Schreiber *et al.*, 1976; Orti Cabo & Shearman, 1977; Garrison *et al.*, 1978; Rouchy, 1982; Dronkert, 1985; Schreiber, 1986). Badenian sulphate sediments of the Paratethys also attract increased interest in the recent years because of their great lithological variability and a rich assemblage of sedimentary structures. The studies on Miocene sulphate sediments in the Carpathian Foredeep continue for more than one hundred years (see reviews by Kwiatkowski, 1972; Garlicki, 1979; Kubica, 1992). The main goal of the author's studies was to restore the history of deposition and diagenesis of Miocene sulphate sediments in the northern part of the Carpathian foredeep

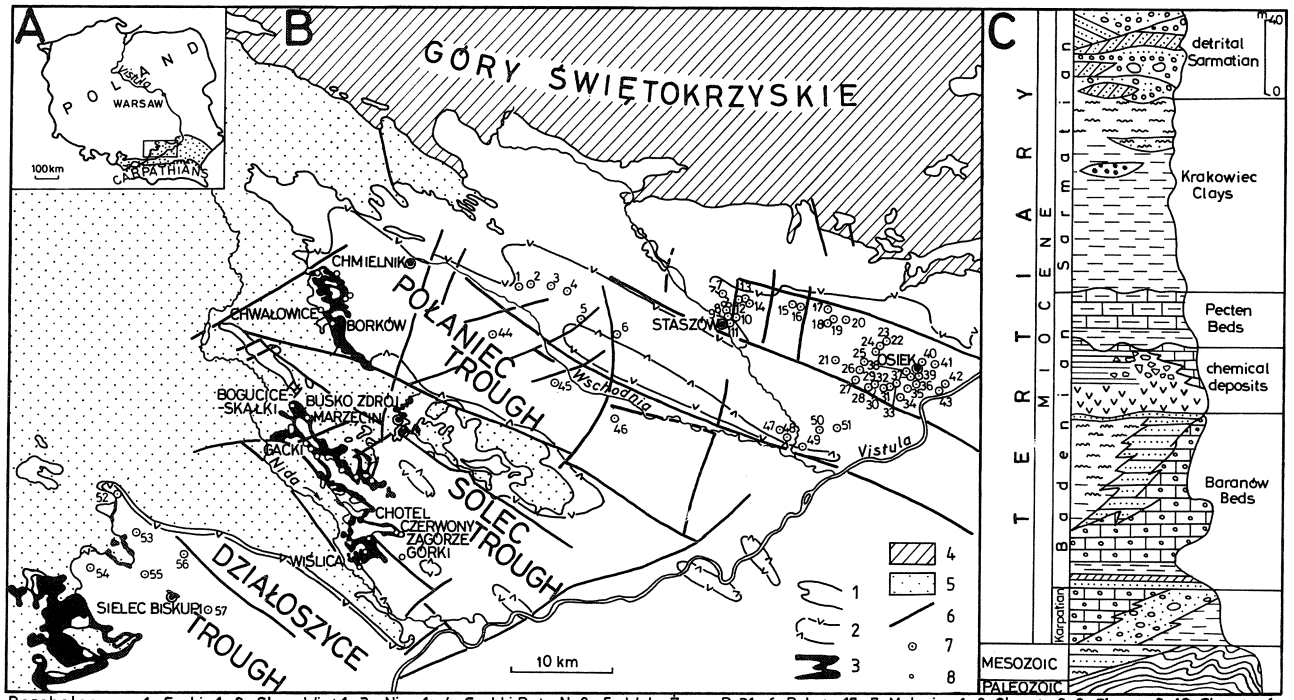

Boreholes: 1-Grabie 1; 2-Stara Wieś 1; 3-Niwa 1; 4-Grabki Duże N-8; 5-Wola Żyzna D-31; 6-Dobrów 17; 7-Maleniec 1; 8-Staszów 2; 9-Staszów 3, 10-Staszów 6; 11-Staszów 5; 12-Pocieszka 3; 13-Pocieszka 4; 14-Pocieszka 2; 15-Wola Wiśniowska 1; 16-Wiśniowa 1; 17-Zawada 1; 18-Czajków 83; 19-Buczyny 1; 20-Wiązownica 1; 21-Strzegom 143; 22-Suchowola 82; 23-Suchowola 81; 24-Suchowola 80; 25-Pliskowola 30; 26-Mucharzów 153; 27-Mucharzów 150; 28-Niekrasów 74; 29-Pliskowola 75; 30-Pliskowola 77; 31-Pliskowola 111; 32-Pliskowola 91; 33-Pliskowola 92; 34-Trzcianka 157; 35-Mikołajów 60; 36-Osieczko 87; 37-Osiek 96; 38-Osiek 61; 39-Osieczko 88; 40-Osiek 156; 41-Osiek 141; 42-Lipnik 98; 43-Lipnik 97; 44-Przyborów 1; 45-Żerniki 1; 46-Strzelce 1; 47-Wymysłów 62; 48-Wymysłów 14/6; 49-Rudniki 23; 50-Okrągła 22; 51-Okrągła 31/9; 52-Ewinów IG-1; 53-Jakubowice IG-1; 54-Pierocice IG-1; 55-Podgaje IG-1; 56-Bieglów IG-1; 57-Kamyszów 1

Fig. 1 Geological map of study area. **A** – extent of Miocene deposits in the Carpathian Foredeep (ZP); **B** – location of studied sections. *1* – limit of Miocene deposits, *2* – limit of sulphate deposits, *3* – gypsum outcrops, *4* – Palaeozoic strata of the Góry Swiętokrzyskie, *5* – Mesozoic strata of the Miechów Trough and of the southern margin of the Góry Świętokrzyskie, *6* – fault, *7* – borehole, *8* – exposure; **C** – general lithostratigraphical column of Miocene deposits south of the Góry Świętokrzyskie

(Fig. 1A) based on a comparison to well studied – as a result of the last decade's research – modern evaporite environments.

The studied area of about 1,100 km^2 (Fig. 1) is situated south of the Góry Świętokrzyskie (in some geological papers referred to as the Holy Cross Mountains) and it includes four sectors with numerous exposures of gypsum and a dense network of boreholes (Fig. 1B): the Nida river area, Staszów area (see Kasprzyk, 1989a), Osiek area, and the Wschodnia river area. The most detailed work was concentrated in these four areas.

The sequence of Badenian sediments in the area of this study begins with lithologically diversified sequence of the so called Baranów Beds (Pawłowski *et al.*, 1985; Fig. 1C). These are followed by chemical sediments which in the northern, peripheral part of the Carpathian Foredeep include gypsum and carbonates. The thickness of gypsum with clayey and carbonate intercalations attains 60 m in local depressions (Pawłowski, 1965; Kubica, 1992). The area of gypsum occurrence is a W-E trending zone up to some tens of kilometres wide. Towards the south, with increasing depth of its occurrence, gypsum is replaced by anhydrite (depths 500 - 2,500 m) which occupies the central part of the Carpathian Foredeep (Kubica, 1972). Salt deposits occur in the southern part of the foredeep, where the evaporite sediments attain their maximum thickness of more than 600 m (Ney *et al.*, 1974; Garlicki, 1979).

The methods of study and the classification of sedimentary structures were based mainly on the papers by Kwiatkowski (1972), Dronkert (1985), Ciarapica *et al.* (1985) and the textbook by Gradziński *et al.* (1986). The petrographic classification by Ciarapica *et al.* (1985) was used for the structures of primary gypsum, the classification of microstructures proposed by Orti Cabo (1977) and Orti Cabo & Rosell-Ortiz (1982) was used for secondary gypsum and anhydrites; nomenclature of Maiklem *et al.* (1969) was applied in the description of anhydrite textures.

GYPSUM LITHOFACIES

The lithological varieties of gypsum (Table 1; Figs. 2-6) reflect its diversified origins; they may be classified in two main groups: (1) primary (crystalline selenitic, massive, and clastic gypsum) (Pls. I-IX: 1, 3; Pl. X: 1) and (2) secondary gypsum (Pl. X: 2). The crystalline selenitic gypsum includes the following lithofacies: glassy, sabre-like, skeletal, and banded with selenite horizons. The other varieties include those of massive gypsum – with crystalline aggregates, stromatolitic, laminated (horizontal or wavy), flaser, alabastrine and nodular, and those of clastic gypsum – gypsoolites, gipsopelites, gypsarenites and gypsorudites.

Table 1

Sedimentary structures in the Miocene gypsum south of the Góry Świętokrzyskie

Sedimentary structures				Description	Occurrence in lithofacies	Position in lithostratigraphical sequence*
Related to crystal growth	Giant blocky crystalline intergrowths	symmetrical vertical asymmetrical vertical assymetrical inclined	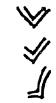	Blocks of parallel subcrystals; flanks of intergrowths symmetrical/asymmetrical to vertical/inclined intergrowth surface	sz	*a*
	Sabre-like selenite crystals			Strongly elongated prismatic crystals with curved upper surface delimited by faces (111), (101), (102)	sa sk	*g, i, m, f*
	Split selenite crystals			Bundles of sabre-like crystals joined at base	sa, sk cl, sl	*g, i, m, b, d, f, r*
	Skeletal selenite crystals			Framework of rod-like prismatic crystals chaotically arranged and intergrown	sk	*f*
	Grass-like selenite horizons			Palisade-like and columnar horizons of prismatic crystals oriented perpendicular to beds	sl, st, sk, sa, sz, cl	*b, d, e, m, l, j, f, r, a*
	Cavoli-type selenite crystals			Domal through cauliflower-like clusters of prismatic crystals arranged in radial bundles	sl, st, cl	*b, d, m, e, j, l, ł, k*
	Crystal growth bands			Streaks of impurities (clay, carbonate, organic matter) parallel to the (120) prism faces	sz, sa, sk, st	*a, g, i, f, m, e*
	Crystalline intergrowths			Sabre-like crystals, interpenetrated or terminating at contact	sa	*g, i, m*
	Gypsum domes			Domal-like structures, up to 12 m in diameter, up to 4 m high, built of radially arranged sabre-like crystals	sa, sk	*g, i, f*
Depositional	Homogenous clastic structure			Homogenised sediment with grain-supported or matrix-supported framework	ga + gp	*n, l, ł*

Sedimentary structures			Description	Occurrence in lithofacies	Position in lithostratigraphical sequence*
Depositional	Millimetric, horizontal/ inclined lamination		Alternations of parallel laminae, 0.03-1 cm thick, differing in mineral composition, colour or grain-size	la, ga, gr, sa, cl, al	*n, p, h, k, ł, m, g, i*
	Centimetric horizontal lamination		Horizontal, parallel laminae, 0.3-1 cm thick, of: gypsum and pelite, pelite, and sandy marl	ga, st	*k, ł, n, m, o, p, l, r*
	Wavy lamination		Alternating wavy laminae of different mineral composition and colour	la, sl, st, sk, cl, sa	*l, k, n, m, j, g, i, b, d, f, o*
	Lenticular lamination		Isolated, irregular and lenticular inserts of laminated gypsum in gypsarenite or pelitic groundmass	fl, la, ga, cl	*h, k, o, m*
	Flaser lamination		Discontinuous laminae of variable thickness, irregular streaks of pelitic sediment	fl, la, ga, gr, st, cl, al	*h, k, l, m, c, g, r, b, j, o*
	Ripples		Small climbing ripples up to 5 mm high (angle of climbing ca. 30°), asymmetrical - symmetry index 4-10	la, ga, fl, st, sl	*k, ł, m, l, h, j, r, b*
	Cross-lamination		Gypsum and clayey-carbonate laminae in sets of flat or herring-bone cross-laminae - angle of dip 15-20°	ga, gr	*o, p, k, h*
	Grading: normal / reverse		Gradual or discrete changes in grain size from 0.01 to 1.0 mm within laminae	la, ga, gr, sl, st, fl, al, sk, cl	*h, k, m, j, n, p, e, c, r, d, b, g*
Erosional	Erosion and (or) dissolution surfaces		Flat and slightly wavy surfaces of discontinuity, often accentuated by a detritic laminae -covered by selenite horizon or partly obliterated by syntaxial crystal growth	sz, sa, sk, sl, st, la, fl, al, ga+gp	*a, c, i, f, b, d, m, j, l, h, n*

Sedimentary structures			Description	Occurrence in lithofacies	Position in lithostratigraphical sequence*
Erosional	Erosional channels		Depressions 1-1.6 cm deep and up to 8 cm wide, trough-like in cross-section; erosion or deformation base; channels filled with gypsum and claystone clasts and clay	ga	*c*
	Pocket-like infillings of clastic sediment		Depressions between corroded and (or) eroded tops of selenite crystals, filled with clastic gypsum or siliciclastic sediment	sa, sl, sz	*a, g, i, m, b, d*
	Sabre-like crystals in reversed position		Strongly elongated sabre-like crystals lying with their curved upper surface down	sa	*i*
Deformational	Distorted bedding		Contorted and broken beds; angular blocks and rick fragments chaotically distributed in fine matrix	gr, ga+gp, st, sl	*n, p, k, o, h, l, j, m*
	Deformation slices		Arcuate fragments of layers and laminae	st, gr	*m, k, l, n, h, l, o, p*
	Turbidite sequence	T_{ABCD}	Bouma sequences, usually incomplete, devoid of upper divisions, repeatedly occurring in section; often sharp bases and gradational tops	ga + gp	*n, p*
	Escape structures		Anticlinal or diapiric swelling of laminated packets with a system of vertical joints	st, sl, la	*d, e, h, m, j, r*
	Dessication-cracks		Network of polygonal cracks in gypsum or clayey-gypsum laminae	sl, st, al	*b, c, j*
	Deformations of laminae below/above selenite crystals		Bending and steepening of laminae above and beneath sabre-like crystals	sl, sa, cl, st, sk	*g, i, m, d, j, b, e, l, h, f*
	Nucleation cone-type load structures		Deformation of laminae beneath selenite clusters; knobby protrusions on the base of selenite layers	sz, sa, sl, cl	*a, g, i, b, d, m, j*

Sedimentary structures			Description	Occurrence in lithofacies	Position in lithostratigraphical sequence*
Deformational	Broken crystals		Fractured or broken crystals with translated or rotated fragments	sa, sk, sl, st	*g, i, m, f, e, d*
	Convolute lamination		Packets of deformed laminae, with deformation gradually dying out upwards or sharply truncated at top and overlain by non-disturbed laminae	ga + gp, la	*n, p, j, h, m*
	Load casts		Deformations of boundary surfaces of gypsum and gypsum-clayey or marly laminae	la	*p*
Biogenic	Cyanobacterial laminites		Parallel lamination, horizontal or wavy; alternation of laminae: gypsum, 0.2-0.8 mm thick, and organic-rich clayey or carbonate, 0.1-0.4 mm thick	st, sl, la, al, no, fl, gp, gr	*e, m, j, l, o, r, c, d, h*, spąg gipsów
	Domal stromatolites		Packets of gypsum laminae: white - microcrystalline and brownish-grey - granular or amoeboidal, bent in dome-like fashion; isolated small, loaf-shaped forms, 2-5 mm high, 3-10 mm wide	st, sl, al, la, cl	*e, m, j, l, r, d, h, k*
	Columnar stromatolites		Columns 1.0-7.2 cm high and 0.8-3.6 cm wide; vertical cross-section - cyllindrical or reversed cone, transverse cross-section - circular or ovate; laminae rectangular or convex	st, sl	*j, l, m*
	Columnar and branching stromatolites		Parallel branching columns (α style)	st	*m*
	Coalescing columnar stromatolites		Two columns covered by one with gently convex laminae	st	*m*
Diagenetic	Nodular		Isolated spherical and ellipsoidal nodules 0.5-2 cm in diameter, embedded in clayey-carbonate matrix	sec, no, al, sl, st, gr, ga	*m, o, r, b, c, d, l, n, e*, i inne

Sedimentary structures			Description	Occurrence in lithofacies	Position in lithostratigraphical sequence*
Diagenetic	Nodular mosaic and mosaic		Aggregated sulphate nodules	no, sec, st, sl, al, gr	*a, b, c, d, e, m, p, l, o*
	Vertically aligned nodular mosaic		Sulphate nodules, vertically or subvertically elongated, several centimetres in diameter, outlined by bituminous clay	sec	*a*
	Layered nodular mosaic		Horizontally elongated gypsum nodules aggregated into nodular layers	no, al, sec, st, sl, fl	*m, o, j, k, b, a*
	Distorted nodular mosaic (enterolithic)		Aggregates and layers of sulphate nodules, closely packed and strongly deformed	sec	*o*
	Crenulated lamination		Packets of finely crenulated laminae with streaks of clayey-organic material	al, st, sl, la	*c, b, e, k, m, o*
	Corroded crystals		Gypsum crystals of irregular outlines	sa, sk, sz, sl, st, cl, gr	*f, g, i, a, m, d, r, b, k, n*
	Rosettes of prismatic crystals		Radial- or chaotic-prismatic aggregates of anhydrite laths	la, sec, a, st, al, sl, sa, sk, i inne	*n, m, o, a, c, d, e, i, f* i inne
	Pseudomorphs after gypsum crystals		Pseudomorphs built of replacive calcite, anhydrite or microcrystalline secondary gypsum	sec, sz, st, la, no	*a, k, n* i inne
	Pseudomorphs after halite crystals		Gypsum pseudomorphs with cement-like fabric	la, fl, st	*n, m, r, o*

* – Lithofacies symbols arranged in order of decreasing frequency

The distinguished lithofacies build up a persistent sequence of eighteen lithostratigraphical units, labelled *a* through *r* (Kasprzyk, 1991; Fig. 7). The lithostratigraphical division is based on that proposed by Wala (1979, 1980) for gypsum sediments in the Nida river area (cf. Kasprzyk, 1991 – Table). Units *a* - *r* have their equivalents also in those sections where gypsum is partly replaced by anhydrite and secondary gypsum (area of the Wschodnia river – Figs. 5, 6; Kasprzyk, 1991).

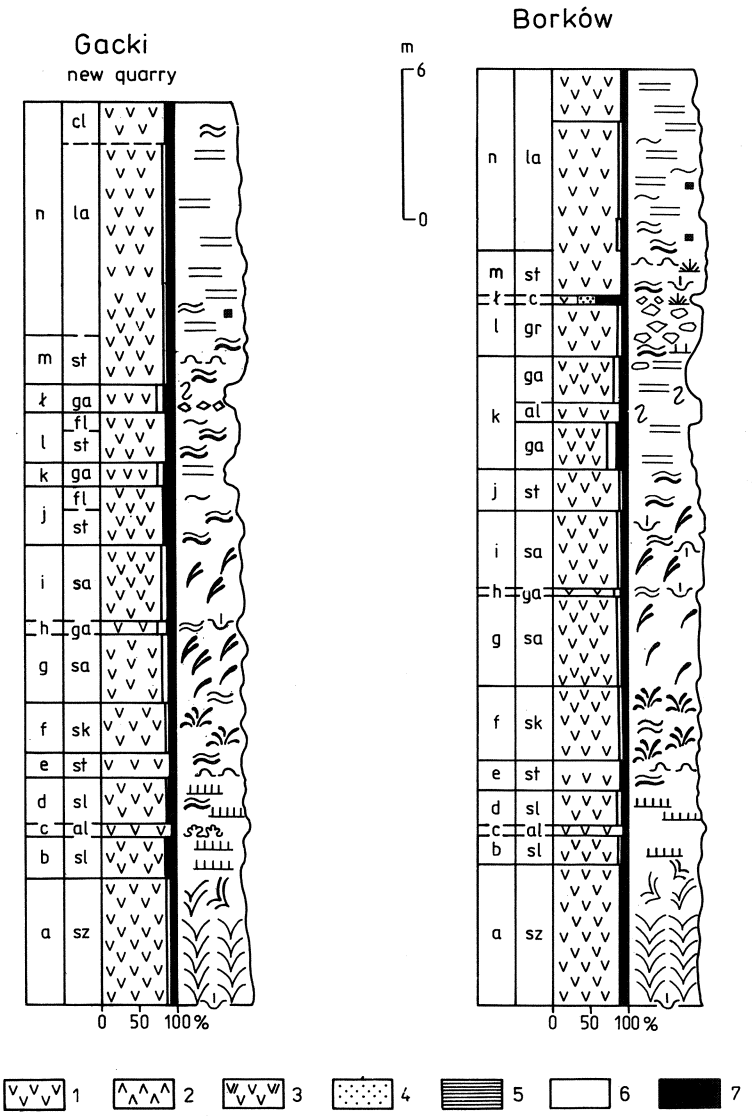

Fig. 2 Lithological-sedimentological columns of gypsum deposits in selected exposures in the Nida area (sections Gacki – new quarry and Borków). *1* – gypsum, *2* – anhydrite, *3* – sulphate rocks in general, *4* – limestones, *5* – dolomites, *6* – carbonate rocks in general, *7* – clays, claystones, mudstones; sz – glassy gypsum, sa – sabre-like gypsum, sk – skeletal gypsum, sl – banded gypsum with selenite horizons, st – stromatolitic gypsum, cl – massive gypsum with crystalline clusters, la – laminated gypsum, fl – flaser gypsum, al – alabastrine gypsum, no – nodular gypsum, oo – gypsoolite, gp – gypsopelite, ga – gypsarenite, gr – gypsorudite, sec – secondary gypsum, a – anhydrite, do – dolomite, c – clay, claystone, s – mudstone, l – limestone, lb – brecciated limestone, (k) – karstic void. For other explanations see Table 1

Crystalline selenitic gypsum

The main constituent of crystalline selenitic gypsum are selenite crystals, of variable form and size, depending on their growth conditions. The specific forms of crystalline aggregates (blocky intergrowths, grass-like aggregates or cavoli) and the sedimentary structures – dissolution and erosion surfaces (Pl. I: 2, 3), load structures (Pl. I: 2), pocket-like infillings with detritic material, detritic laminae, and stromatolitic structures (Pl. IV) – suggest a primary origin of gypsum, in a shallow subaqueous environment of highly concentrated brine (Warren, 1982; Schreiber *et al.*, 1982; Orti Cabo *et al.*, 1984; Schreiber, 1986; Bąbel, 1986, 1987 and references therein). Thin intercalations of massive or clastic gypsum indicate episodic changes in the conditions of crystallization and sedimentation.

Glassy gypsum (sz – szklica gypsum in Polish) is distinguished among the selenitic gypsum varieties by its spectacular crystal form (Kwiatkowski, 1972, 1974; Wala, 1979; Kubica, 1985; Bąbel, 1984; 1987; Kasprzyk, 1989a). It is built of giant (up to 3.5 m high) blocky crystalline intergrowths Pl. I-II. The aggregates of parallel intergrown crystals are arranged symmetrically on the opposite sides of a vertical or subvertical cleavage surface, which is also the composition surface of crystal intergrowth (Bąbel, 1987, 1990; Pl. II: 1). The crystals in both flanks of the intergrowth maintain the basic features of selenite growth, such as: splitting, bending of upper surfaces, and zonal growth of prismfaces (120) delineated by streaks and laminae of mineral and organic inclusions (clay and calcite aggregates, cyanobacterial filaments). The clayey-carbonate streaks distributed along the curved surfaces of the split crystalline segments represent the sediment that was preferentially trapped and accumulated on the surfaces which passively participated in the process of crystal growth (cf. Orti Cabo *et al.*, 1984).

The intergrowth surface has a relief related to the blocky structure of the intergrowth flanks (Pl. II: 1). Asymmetrical intergrowths up to 1.5 m high, whose intergrowth surface is slightly or strongly inclined, occur in the upper part of the glassy gypsum complex. Their upper, better developed flanks often include a second generation of smaller intergrowths (up to 0.5 m high) (Pl. II: 2, 3). They show irregular zig-zag contact surfaces and reduced widths of their flanks due to competitive growth. Surfaces of dissolution and(or) erosion (Pl. I: 2, 3) correlate over a distance of more than ten kilometres, indicating palaeorelief of the upper surface of the selenite layer at a certain stage of its growth (cf. Warren, 1982; Bąbel, 1984, 1987).

Flat-walled intercrystalline voids, often covered with fine lenticular crystals up to 2 cm in diameter, occur within the intergrowths, especially at their tops and in the outer parts of their flanks. The shapes of these voids indicate their synsedimentary origin.

The giant blocky crystalline intergrowths grew at the basin bottom (cf. Bąbel, 1987); the growth has taken place under relatively stable conditions of

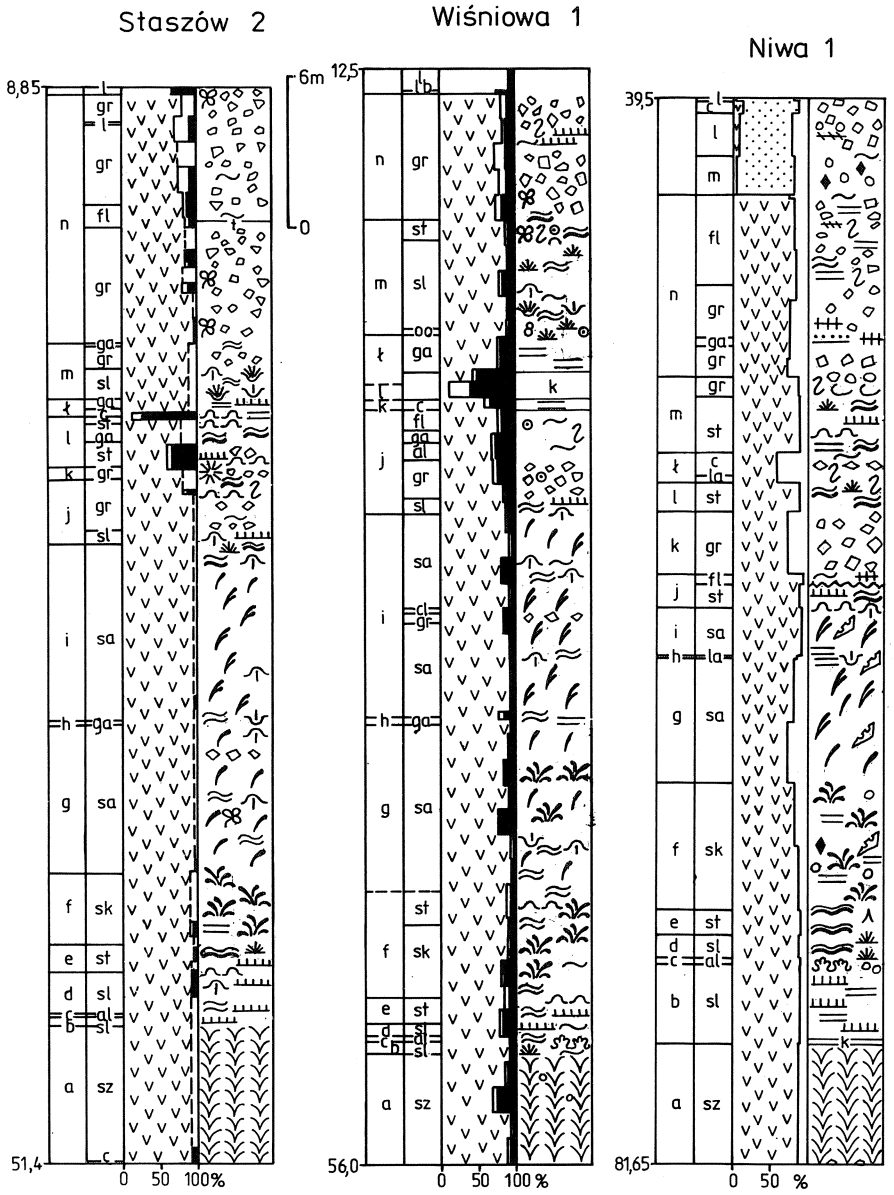

Fig. 3 Lithological-sedimentological columns of gypsum deposits in selected boreholes in the Staszów area. The interpretation includes: *solid line* – petrographical and chemical composition, *dashed line* – petrographical composition. Other explanations see Fig. 2

salinity, depth and water dynamics. The discontinuity (dissolution) surfaces and the streaks of impurities record small variations in water salinity and fluctuation or vanishing of halocline, similarly as in modern salinas of southern Australia (Warren, 1982, 1983). Competitive growth of neighbouring in-

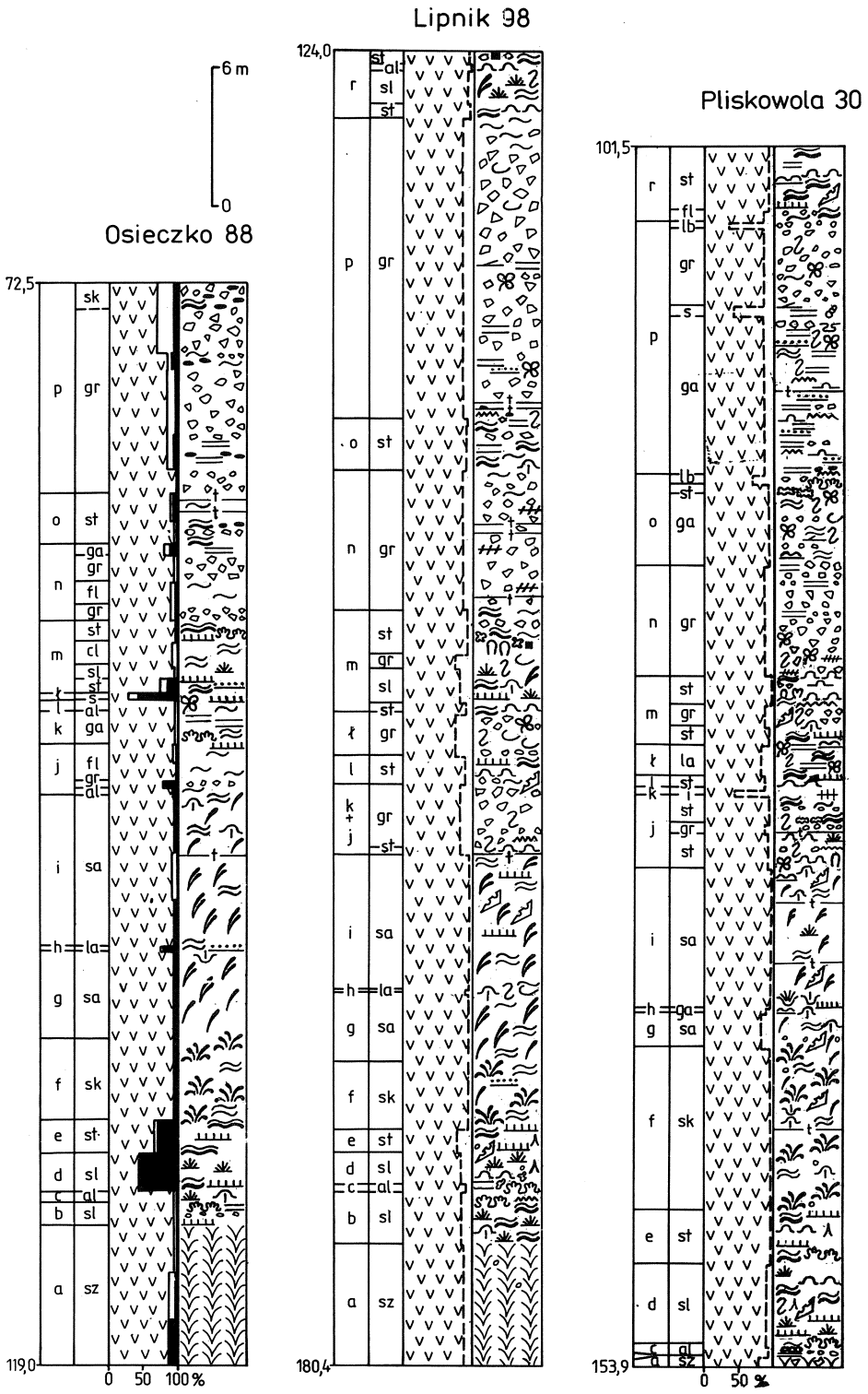
Osieczko 88
6 m
0
72,5
119,0
0 50 100 %
Lipnik 98
124,0
180,4
Pliskowola 30
101,5
153,9
0 50 %

tergrowths controlled the development of the vertical asymmetrical forms (Pl. II: 2, 3). The inclined intergrowths grew as isolated forms under conditions of increased water dynamics. In the inclined position, the growth of the upper flank was favoured and of the lower one – hindered.

Similar structures occur in extremely coarse-crystalline selenitic gypsum in modern coastal salinas of southern Australia (Goto, 1968; Warren, 1982, 1983; Kendall & Warren, 1988). There the middle part of gypsum sediments includes crusts of great (up to 2 m high) vertically oriented selenite crystals with irregular, millimetric lamination. These great crystals, related to shallow (less than 10 m) waters of periodically changing salinity, are a modern equivalent of the Badenian glassy gypsum.

Sabre-like gypsum (sa) is distinctive by the presence of strongly elongated sabre-like crystals (Pawłowska, 1962; Kwiatkowski, 1974; Wala, 1979; Kubica, 1985; Bąbel, 1986; Kasprzyk, 1989a, b; Pl. III: 1-3). The sabre-like selenite crystals are 15 - 90 cm long and show characteristic features: splitting (Pl. III: 2), regular growth zones, and curvature of the upper surfaces (Pl. III: 2, 3) due to a torsion of the crystalline lattice (Bąbel, 1986). Crystals were deformed during their growth on the bottom in the presence of organic matter (cf. Cody, 1976; Orti Cabo & Shearman, 1977; Schreiber, 1986). Organic and mineral impurities hampered the growth of crystals on the curved surfaces. The sabre-like selenite crystals grew competitively by expansion of prism faces (120) or clusters of parallel intergrown rod-like prismatic crystals (Orti Cabo *et al.*, 1984; Bąbel, 1986), which determined the elongated form and the characteristic growth structures.

The sabre-like crystals are variously distributed in the rock. The most commonly, especially in the upper part of the gypsum sequence, they have uniform orientation (Pl. III: 3). In the Nida river area their inclination to the north and northeast was recorded in most exposures along a line several kilometres long (Bąbel, 1986). The sabre-like crystals that build gypsum domes are oriented radially (Pl. III: 1, 2). The gypsum domes are megastructures up to 12 m in diameter and up to 4 m high, exposed in the Nida region (Bąbel, 1986 and references therein). The structure of the domes includes a distinct core, up to 5 m across, built of skeletal gypsum and selenite clusters of *cavoli* type. The core is surrounded by deformed layers of sabre-like gypsum, 0.3 - 0.5 m thick. The sabre-like crystals are strongly elongated (up to 90 cm) and intergrown (Pl. III: 2). Bedding is obliterated in the flanks of the domes by syntaxial growth of subhorizontally oriented elongated crystals. The gypsum domes occur isolated or in groups. Their origin is the subject of a long-lasting discussion. By the analogy of their form to the gypsum domes that form contemporaneously in coastal salinas of southeastern Spain and southern Aus-

Fig. 4 Lithological-sedimentological columns of gypsum deposits in selected boreholes in the Osiek area. Explanations see Figs. 2 and 3

tralia (Warren, 1982, 1983; Orti Cabo *et al.*, 1984; Kendall & Warren, 1988), they may be regarded as synsedimentary structures formed on substrate elevations due to preferential growth of crystals.

The space between the sabre-like crystals is filled with finer selenites crystals, up to 10 cm long. They are oriented perpendicularly and geopetally to the curved surfaces of the sabre-like crystals, or distributed chaotically in a clayey-carbonate-gypsum matrix (Pl. III: 3) locally strongly contaminated with organic matter.

Sabre-like gypsum forms a unit up to 5 m thick with distinct intercalations of laminated or flaser gypsum, clastic gypsum and pelitic interlayers. The sabre-like crystals load-deform underlying laminae underlying (cf. Bąbel, 1986; Kasprzyk, 1989a). Similar load structures are described from gypsum deposits of the Mediterranean region as *nucleation cones* (Dronkert, 1976, 1985; Lo Cicero & Catalano, 1976) or *mamelloni* (Vai & Ricci Lucchi, 1977); they were also recognized in secondary gypsum, preserving primary structures of selenite, in Eocene of Catalonia (Busquets *et al.*, 1985). Bending and oversteepening of laminae over the selenite crystals, observed in the Badenian gypsum, is due to compaction (cf. Hardie & Eugster, 1971; Dronkert, 1985; Bąbel, 1986). The elongated crystals were especially susceptible to breakdown during compaction and to penesyndepositional dissolution and mechanical abrasion (Dronkert, 1985; Schreiber, 1986). Sabre-like crystals in reversed position have been observed in the top part of unit *i*; they record a change in hydrodynamic regime in the basin and terminate the subaqueous sedimentation of selenite gypsum (Kasprzyk, 1991).

Selenitic lithofacies with sabre-like crystals are known from modern coastal salinas of southeastern Spain and southern Australia (Warren, 1982; Orti Cabo *et al.*, 1984) where they form dome-like selenite crusts.

Skeletal gypsum (sk) (Pawłowska, 1962; Kwiatkowski, 1972, 1974; Kubica, 1985, 1992; Wala, 1974, 1979) is built of rod-like to prismatic selenite crystals up to 15 cm long, chaotically distributed and mutually intergrown (Pl. III: 4). Twins along (100), asymmetrical with the lower flank poorly developed or reduced, are common. The space between selenite crystals is partly filled with granular and microcrystalline gypsum rich in carbonate and pelitic-organic material. Skeletal gypsum occurs in layers, 0.2 - 2.5 m thick, intercalated with massive and clastic gypsum laminae, locally graded.

It also builds central parts of the gypsum domes (Pl. III: 1, 2). Clusters of crystals, similar to those described above, form the cores of the gypsum domes that are forming now in coastal salinas (Warren, 1982; Orti Cabo *et al.*, 1984; Kendall & Warren, 1988).

Banded gypsum with selenitic horizons (sl) is a widely distributed lithofacies. Stratification consists in alternation of layers of selenitic gypsum and massive (laminated, alabastrine and stromatolitic) or clastic gypsum (Pl. IV). The boundaries between successive selenite horizons are in some cases indistinct, marked only by a thin pelitic lamina or a gradation in crystal size.

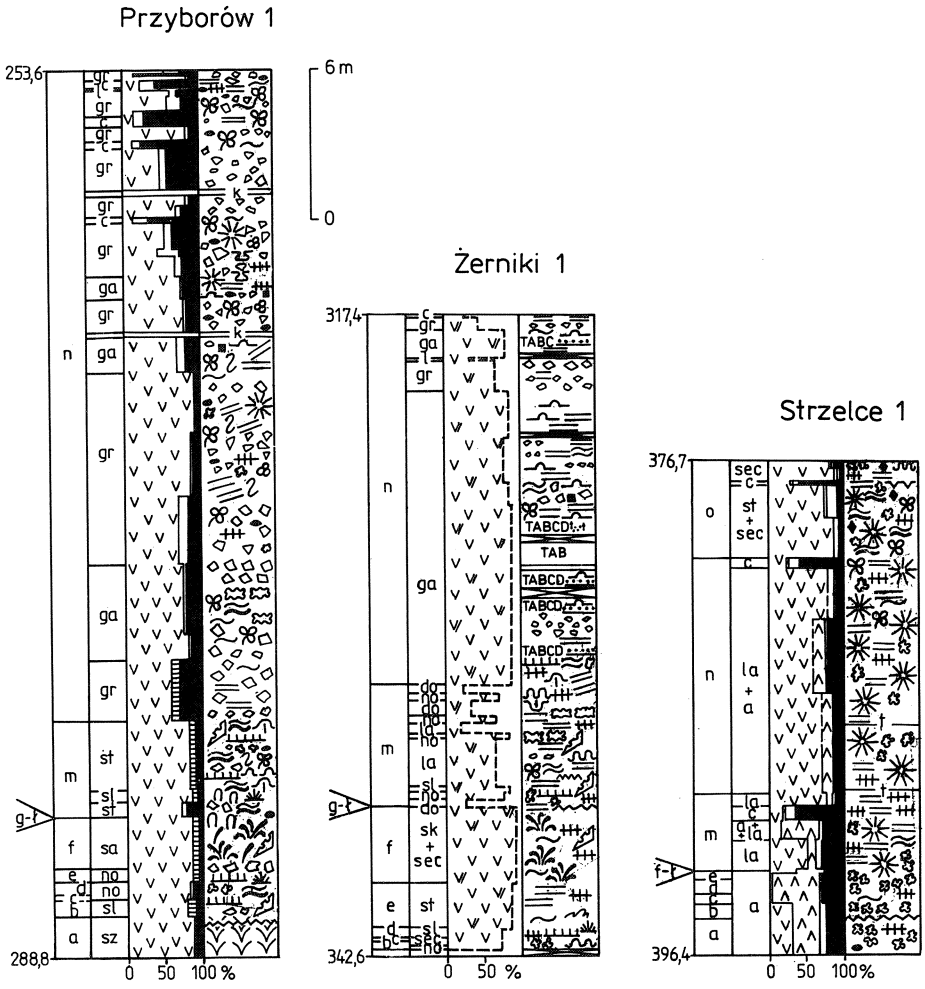

Fig. 5 Sections of sulphate deposits in boreholes Przyborów 1, Żerniki 1 and Strzelce 1 situated in the Wschodnia river area. Explanations see Figs. 2 and 3

Selenite crystals, up to 25 cm high, are oriented vertically or radially and perpendicular to the stratification. They form palisade and grass-like structures or domal, rosette and cauliflower-like forms of cavoli type (Pl. IV: 2). The grass-like and cavoli structures were first described by Richter-Bernburg (1973) from the Messinian gypsum of Sicily. Crystalline clusters of cavoli type – in contrary to grass-like aggregates – do not form continuous horizons and they have grown preferentially on substrate elevations (Pl. IV: 2). Schreiber *et al.* (1976, p. 742) explain their origin in the Messinian gypsum by increased density of nucleation and competitive growth of crystals.

The other distinctive sedimentary structures in banded gypsum include pocket-like hollows between the corroded or eroded apices of selenite crys-

tals, infilled with detritic material, stromatolitic structures, traces of dissolution and erosion of crystals, load structures of nucleation-cone type, brecciated horizons and desiccation cracks.

Horizons of selenite crystals of grass-like and cavoli type are characteristic forms of selenite crusts in Quaternary sediments of coastal salinas in SE Spain and in southern and western Australia (Arakel, 1980; Warren, 1982; Orti Cabo *et al.*, 1984; Dronkert, 1985; Logan, 1987). They also form temporarily in shallow (up to 0.5 m) hypersaline waters in canals draining sabkha area at the coasts of the Persian Gulf (Gunatilaka & Shearman, 1988). Pelitic-carbonate or organic laminae in the selenite horizons record changes in salinity, dynamics and depth of water.

Massive gypsum

Massive gypsum is a rock in which the proportion of selenite and other macrocrystalline forms of gypsum does not exceed 50 percent. Several lithofacies of massive gypsum could be distinguished on the base of their lithological, petrographical and sedimentological characteristics.

Massive gypsum with crystalline clusters (cl) is a transitional variety between crystalline selenite and massive gypsum. Selenite crystals, up to 25 cm long, occur in aggregates – common are twins along (100), grass-like horizons or cavoli – and in single crystals chaotically distributed in the background of microcrystalline and granular gypsum. The background displays planar or irregular lamination with pelitic-carbonate material. Deformation of laminae (load structures) beneath selenite clusters proves their primary nature (cf. Dronkert, 1985; Bąbel, 1986) and permits their distinction from recrystallization forms common in the microcrystalline background. Fine lenticular gypsum crystals (up to 2 mm in diameter) probably originated early during diagenesis by growth in gypsum mud (cf. Schreiber, 1986). Primary outlines of crystals were partly or completely obliterated by diagenetical modifications including reduction, dissolution and recrystallization, similarly as in modern evaporite environments (Logan, 1987).

Stromatolitic gypsum (st) is a lithofacies (Pl. IV: 1; Pl. V) whose development reflects the intensity and relations of two superimposed processes: cyanobacterial activity and chemical precipitation of gypsum. Stromatolite structures have been hitherto described only from the lower part of the gypsum sequence (Kwiatkowski, 1972; Schreiber, 1978; Wala, 1979, 1980; Kubica, 1985, 1992; Niemczyk, 1988b; Kasprzyk, 1989a). The present author's studies revealed that stromatolitic gypsum occurs at various positions in the sequence, in layers 0.3 - 3.2 m thick (Figs. 2-6). Their common feature is the presence of well preserved organic structures such as stromatolites and cyanobacterial laminites whose morphological and microstructural variety permits the distinction of several types of stromatolitic gypsum (Kasprzyk, 1993).

Laminated gypsum (la) is differentiated with respect to its lithology and

origin. The lamination is expressed by alternating gypsum laminae: light, 0.1 - 3.0 mm thick, only slightly contaminated with clay and carbonates, and dark laminae, 0.01 - 0.5 mm less frequently up to 1 mm thick, containing a greater admixture of pelitic and carbonate material. The variation in chemical composition is reflected in the varying colour of laminae. In thin section the laminae reveal microcrystalline or granular structure; clay and carbonate minerals are usually dispersed. Parallel orientation of crystals, sometimes with traces of corrosion and (or) abrasion, is especially well marked in pelitic or gypsum-marly laminae. The inclination of laminated sets usually does not exceed 8°, but exceptionally it may attain even 45°. Besides parallel lamination (horizontal or wavy – Pl. VII: 2; Pl. IX: 3), there occur also lenticular, flaser, crenulated and convolute lamination. The disturbed, folded laminae often are thinned or swelled in the fold hinges. A large variation in the fold styles is present within sets of laminae (Kwiatkowski, 1972). Parallel lamination is often accentuated by normal or reversed gradation within laminae. Laminated gypsum occurs in both, thin layers of a few centimetres, and in beds up to 9 m thick.

The origin of the studied laminated gypsum is referred by the author to periodical, not necessarily seasonal, variations in water chemistry and halocline fluctuations. Redeposition of gypsum sediment in shallow and deep (below wave base) subaqueous environment could play a role. In this case, diagenetic processes including dissolution and recrystallization completely obliterated or modified the structural and textural features typical of clastic sediment.

Shallow-water laminated gypsum is a facies widely distributed in modern salinas and sabkhas (Arakel, 1980; Warren, 1982, 1983; Schreiber, 1988; Kendall & Warren, 1988; Gunatilaka & Shearman, 1988).

Flaser gypsum (fl) displays indistinct lamination, locally obliterated and discontinuous, expressed by the presence of irregular bands and flasers distinguished from the microcrystalline or granular background by their darker colour and rich pelitic admixture. Gypsum crystals within these bands and flasers display usually parallel orientation and traces of corrosion and abrasion. Kwiatkowski (1972) included this variety of gypsum to banded alabaster with relic lamination, and explained its origin by spontaneous liquefaction of laminated sediment during early diagenesis. Flaser gypsum with graded bedding has – in the present author's opinion – synsedimentary origin, related to current deposition.

Alabastrine gypsum (al) is macroscopically a cryptocrystalline massive rock, cream-coloured, light grey or beige, with distinctive finely crenulated lamination (Pl. IV; Pl. VII: 1). It occurs usually in thin layers, 0.1 - 0.5 m thick, with sharp boundaries and irregular, dome-like to cauliflower-like tops (Pl. VII: 1), sometimes covered with a thin horizon of selenite crystals up to 5 mm high of cavoli-type morphology. Locally they are overlain by clayey-gypsum rhythmite with characteristic structures – horizons of brecciated gypsum

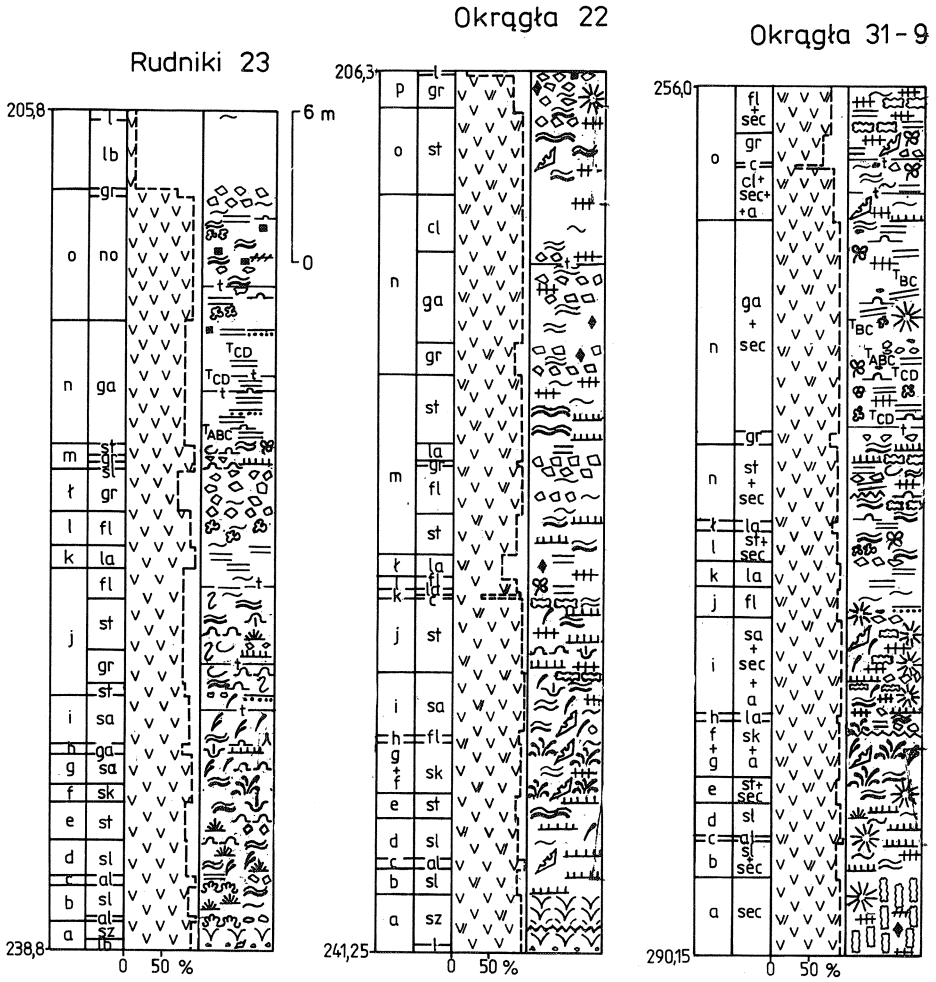

Fig. 6 Sections of sulphate deposits in boreholes Rudniki 23, Okrągła 22 and Okrągla 31-9, situated in the Wschodnia river area. Explanations see Figs. 2 and 3

laminae, mud-cracks, erosional channels (Pl. VII: 1) indicating periodic emergence (cf. Schreiber *et al.*, 1982). Another form are irregular nodular layers and patches of alabastrine gypsum within the matrix in selenite gypsum. Recrystallization effects are common within these patches.

Alabastrine gypsum, similar to that described above, is known from sediments of modern coastal salinas and sabkhas (Warren, 1982, 1989; Orti Cabo *et al.*, 1984; Warren & Kendall, 1985; Purser *et al.*, 1987). A 30-cm thick layer of finely crystalline gypsum (gypsum mush – Warren & Kendall, 1985) is present in the sequence of sabkha sediments of the Persian Gulf. It is built of fine, up to 2 mm across, lenticular gypsum crystals growing early during diagenesis within a microbial mat in the intertidal zone. The resulting sedi-

ment, preserving only relics of original lamination, is very similar to the alabastrine gypsum accompanying the studied Badenian stromatolitic lithofacies. A modern facies equivalent of the alabastrine gypsum is also a finely crystalline (crystal diameters < 0.06 mm) gypsum sediment (*gypsite*), terminating the sedimentary sequence in coastal salinas of southern Australia (Warren, 1982). This sediment is a result of multiple phases of dissolution of gypsum crystals during intermittent subaerial exposure and of precipitation of gypsum from brine in vadose zone.

Nodular gypsum (no) is a rock whose distinctive feature is the presence of spheroidal and ellipsoidal nodules 1 to 12 cm in diameter (cf. Maiklem *et al.*, 1969). The nodules occur within a clayey-carbonate matrix, isolated or in aggregates and layers up to 20 cm thick. Individual nodules and their aggregates are sometimes contorted, forming enterolithic structures, or spread in irregular, horizontally extensive bands. Inner parts of the nodules are built of microcrystalline, granular and irregularly cloudy gypsum, surrounded by an aureole of lenticular crystals (up to 0.4 mm in diameter) concentrically oriented. Microcrystals of calcite and dolomite occur dispersed. Internodular space is filled with dolomicrite, clay minerals and organic matter; they are sometimes accompanied by quartz and celestite. Parallel or wavy lamination is common within the matrix, it is marked by the presence of discontinuous, wedging out or nodular laminae up to 2 mm thick, composed of lenticular and granular gypsum. The lamination is accentuated by streaks of clay and organic matter, distinctly bent around the gypsum nodules.

The Badenian nodular gypsum consists of fine (up to 2 mm in diameter), single or aggregated gypsum nodules, interpreted by the author as early diagenetic, formed in subaerially exposed environment of sabkha type (cf. West *et al.*, 1979), as well as from greater, vertically or horizontally elongated nodules of secondary gypsum (Pl. X: 2), genetically related to the transformations of crystalline selenite gypsum (Kasprzyk & Orti Cabo, in prep.).

Clastic gypsum

Clastic gypsum includes varieties with structural and textural features characteristic of terrigenous material (Hardie & Eugster, 1971; Arakel, 1980). They formed by mechanical remobilization of gypsum sediment and its redeposition. The clastic gypsum includes a marked proportion (15 - 50 weight percent) of terrigenous material – clay minerals, quartz, micas, feldspars, rock fragments and coalified plant debris. The grains include also macrofaunal and microfaunal bioclasts and sporadically ooids. The clasts vary in their degree of rounding and sorting as well as in shape (discoidal, elliptic, spherical, rod-like) and dimension (0.1 - 50 mm), depending on the intensity of the processes of physical abrasion, dissolution and crystallization in a high-energy environment (cf. Logan, 1987). Clasts of gypsum rocks are also common. The long axes of the clasts are often oriented parallel to bedding.

The varieties of clastic gypsum include: gypsoolites, gypsum pelites, gypsarenites, and gypsorudites.

Gypsoolites (oo) have been found in the upper part of the gypsum sequence as a layer 28 cm thick in banded gypsum with selenite horizons (Fig. 3; Kasprzyk & Bąbel, 1986). Detritic sediment with ooids fills also spaces between selenite crystals in the underlying beds. Gypsoolites are built of gypsum ooids, 0.7 - 2 mm in diameter, representing various morphological forms and genetically related to an environment of variable salinity and water dynamics (Bąbel & Kasprzyk, 1990).

Gypsopelites (gp) have pelitic structure with dominant grain-size fraction below 0.06 mm. These rocks occur mostly in thin (up to few tens of centimetres) layers with homogeneously clastic structure, rarely with graded bedding and flaser, lenticular or convolute lamination (Pl. IX: 1). Convolute lamination is characteristic of turbidite sequences and other laminated sediments, whose rapid deposition makes them susceptible to spontaneous liquefaction. They packets of deformed laminae gradually flattening towards the top or sharply truncated by overlying non-folded lamina (Pl. IX: 1). Similar disturbances and deformations of laminae in laminated gypsum in the southern margin of the Góry Świętokrzyskie were described as "folds" (Kwiatkowski, 1972) or "flowage-fold structures" (Kubica, 1992). Kwiatkowski (1972) attributed their origin to thixotropic liquefaction of laminae within a laminated package during early diagenesis. Brecciated horizons and algal laminites with calcified cyanobacterial filaments, observed in gypsopelites, record periods of water agitation and freshening. The gypsum clasts are reworked (corroded and abraded) crystals, which occur in clusters or dispersed in clayey-marly matrix locally rich in peloids and coalified plant debris.

Clastic, fine-grained (< 0.06 mm) gypsum sediments were described from modern coastal salinas of western Australia (Arakel, 1980; Logan, 1987; Kendall & Warren, 1988). These sediments show distinctive sedimentary structures – lamination, ripples, cross-lamination, graded bedding, and they occur together with other varieties of clastic gypsum.

Gypsarenite (ga) is – according to Arakel (1980), Warren (1982) and Schreiber (1986) – a variety of clastic gypsum with dominant fraction of 0.06 - 2 mm. Gypsarenites occur in massive or stratified beds 0.1 - 11.5 m thick. The gypsum clasts are strongly abraded and corroded crystals or their fragments (Pl. VIII: 4). The granular components are set in gypsum-clayey-carbonate matrix. Structures of gypsarenites are homogeneous or laminated . The types of lamination include millimetric parallel lamination – horizontal or wavy – and centimetric horizontal lamination, consisting of alternating laminae of gypsum and pelite or marly sand (clayey gypsum-rhythmite – Kasprzyk, 1989a; Pl. VII: 1, 2). Lenticular, flaser and convolute lamination is also common (Pl. VIII: 1; Pl. IX: 1). Frequent are: folding and fracturing of laminated packets, graded bedding (Pl. VII: 2, 3), ripples as well as turbidite sequences, usually incomplete and devoid of the upper division. More com-

plete T_{ABCD} sequences, up to 60 cm thick, occur in the area of the Wschodnia river (Fig. 5). The turbidite sediments include load casts related to thixotropic liquefaction of laminated sediment in a system with unstable density stratification. Alternating laminae pure and rich in clayey-carbonate impurities formed a trigger system in which liquefaction – not spontaneous but mechanically triggered by a storm, earthquake or alike – occurred selectively in pure gypsum laminae (see Kwiatkowski, 1972). The impure laminae were less susceptible to liquefaction and sunk in the liquefied laminae, forming characteristic, tight depressional structures, flame and load structures, described from the Messinian sulphate turbidites of Sicily (Catalano *et al.*, 1976). All these structures indicate that gypsarenites originated by mechanical remobilization and redistribution of clastic gypsum sediment (cf. Garlicki, 1980; Schreiber, 1988).

Lithofacies of fine-grained and medium-grained gypsum (grains < 2 mm in diameter) are known from sediments of modern salinas and sabkhas on the coasts of Australia, Spain, USA and Egypt (Arakel, 1980; Warren, 1982; Orti Cabo *et al.*, 1984; Schreiber, 1986; Dronkert, 1985). Gypsarenites in salinas of southern and western Australia form due to the action of waves and (or) wind by mechanical remobilization of shallow water or emerged sediments; they are a modern equivalent of the fossil gypsarenites.

Gypsorudites (gr) consist of broken gypsum crystals, clasts of gypsum, carbonate and argillaceous rocks (up to 15 cm long), and bioclasts, which form the skeletal framework dispersed in gypsarenite matrix (Pl. VIII: 1-3). Peloids, fragments of cyanobacterial filaments and coalified plants, as well as lenticular gypsum crystals (up to about 0.5 mm in diameter) occur within the matrix. Gypsum crystals have traces of corrosion and abrasion (Pl. VIII: 3, 4) and are often oriented parallel around greater rock fragments. The degree of rounding of the grains is variable, depending of the environment of deposition. The gypsorudites which occur in thick beds, up to 12.9 m in thickness, display disturbed bedding, deformational slabs, fragmented and folded layers and laminae as well as matrix-supported fabric.

Gypsorudites were described from various evaporite formations. Most authors relate their origin to mechanical remobilization and redeposition of clastic material by subaerial or subaqueous mass movements (e.g. Meier, 1975; Schlager & Bolz, 1977; Richter-Bernburg, 1985; Kubica, 1985, 1992; Niemczyk, 1988a, b).

INTERPRETATION OF SEDIMENTARY ENVIRONMENT

Palaeogeography at the onset of sulphate sedimentation

The evaporite basin of southern Poland, which formed at the foreland of the Carpathians during the Badenian time, was bordered by barriers and featured by a zonal distribution of facies. Sulphate deposits were laid down on a

shallow shelf while rock salt formed in the narrow deepest part of the basin (Garlicki, 1979). The extent and nature of evaporite deposition were controlled by climatic and tectonic factors, which determined palaeogeographical conditions within the basin, such as substrate relief, water depth and salinity.

The deposition of the Baranów Beds largely levelled the morpho-structural relief of the sub-Miocene substrate, though algal "reefs" growing on elevations emphasized the pre-existing relief. It is probable that these areas, now devoid of sulphate deposits, were already emergent during the deposition of evaporites in the central part of the basin (cf. Wilczyński, 1984; Studencki, 1987; Kasprzyk, 1991, fig. 8).

Table 2

Diagnostic features of sabkha environment

environment	subaerial* peritidal zone
climate	arid
supply	rainfall, supply: a/ surficial* (rivers, sea-water flooding by tides or storm, winds) b/ subsurface* (percolation of sea water) c/ underground (continental groundwater)
diegenesis	– growth of sulphate minerals*: *in situ* replacement and displacive growth – nodular structures* and enterolithic structures* – lenticular gypsum crystals*, dispersed or in clusters in biogenic sediment
evaporitic minerals	gypsum*, anhydrite*, halite*
other replacing minerals	dolomite*, celestine*, magnesite

* – features present in the studied sediments

The sulphate deposits were laid down at the front and below the elevations of the carbonate shelves, partly covering the Lithothamnium sediments. The bottom surface, inherited after the deposition of the Baranów Beds, displayed a slight (< 1°) southward or southeastward inclination, characteristic of ramps (cf. Read, 1985). The facies variation of the sulphate deposits reflects the relief of the ramp. At the beginning of evaporite sedimentation the southern slopes of the Góry Świętokrzyskie were occupied by a system of extensive shallow-water lagoons separated by NW-SE trending island barriers or shoals (Kasprzyk, 1991, fig. 3). The facies variation permits the distinction of the following palaeogeographic zones: 1) sabkha-like coastal salt flats, 2) lagoons (salinas) forming a system of interconnected shallow, more or less isolated, evaporite basins, 3) islands devoid of evaporite sedimentation (carbonate shelves), 4) outer shelf – wide zone directly connected with the open basin.

Sabkha has been variously interpreted and defined in the literature (Handford, 1981; Purser, 1985; Warren, 1989), nevertheless there is a consensus on the structural and textural characteristics as well as mineral composition of sabkha sediments and the assemblage of diagenetic processes (Table 2), which are distinctive for the modern sabkha. This assemblage may be also recognized in the Badenian sulphate deposits south of the Góry Świętokrzyskie (Table 2). Typical sabkha sediments are nodular gypsum and anhydrite with abundant pelitic-dolomitic matrix (Pl. IX: 2); their origin in a diagenetic environment of sabkha is confirmed by the results of isotopic analyses: the values of $\delta^{18}O$ in dolomite are 3.15 and 3.50 permill (cf. Hałas, 1982; Pierre, 1988).

Sabkha formed in the studied area in Badenian time, at the initial stage of evaporite sedimentation, on the southern slope of a NW-SE extending central elevation (Kasprzyk, 1991, fig. 3). The salinas occupied an extensive area of subaqueous deposition and communicated with the open sea through a zone of outer shelf.

Evolution of sulphate sedimentation

The uniformity of gypsum lithofacies over the large area of the southern margin of the Góry Świętokrzyskie indicates uniform environment and a similar evolution of sedimentation. In this area sulphate sedimentation began in coastal lagoons, partly isolated from the open sea by a system of carbonate barriers, inherited after the deposition of the Baranów Beds (Kasprzyk, 1991, fig. 8). Lenticular gypsum crystals grew in local depressions of the bottom, within black clays, thus forming the basal biolaminites (Pl. V).

The gypsum sequence begins with glassy gypsum (unit *a*, Fig. 7), laid down in conditions similar to those in modern coastal salinas of southern Australia (Goto, 1968; Warren, 1982, 1983; Kendall & Warren, 1988). Conditions favourable for the growth of the great crystalline intergrowths existed in calm, density-stratified highly saline waters. The streaks of impurities as well as dissolution and erosion surfaces in the glassy gypsum prove that its growth was periodically interrupted or slowed down due to increased supply of fresh water and halocline fluctuations.

The growth anomalies, such as inclined intergrowths (Pl. II: 2, 3), laminae of detritic gypsum, grass-like selenite horizons, or a large proportion of impurities, which are observed in the upper part of the glassy gypsum, indicate a change in the conditions of deposition: increased dynamics of water, and greater changes in salinity.

A sea level drop, probably related to eustatic movements or evaporation in connection with the shallowing due to the increase of sediment fill, as well as the decrease in salinity, impeded the development of glassy gypsum. The varying sedimentary conditions are recorded in alternating selenite crystals and microbial mats (Fig. 7). It is probable that cyanobacterial mats, which bound and stabilized detritic gypsum sediment, were completely gypsified in

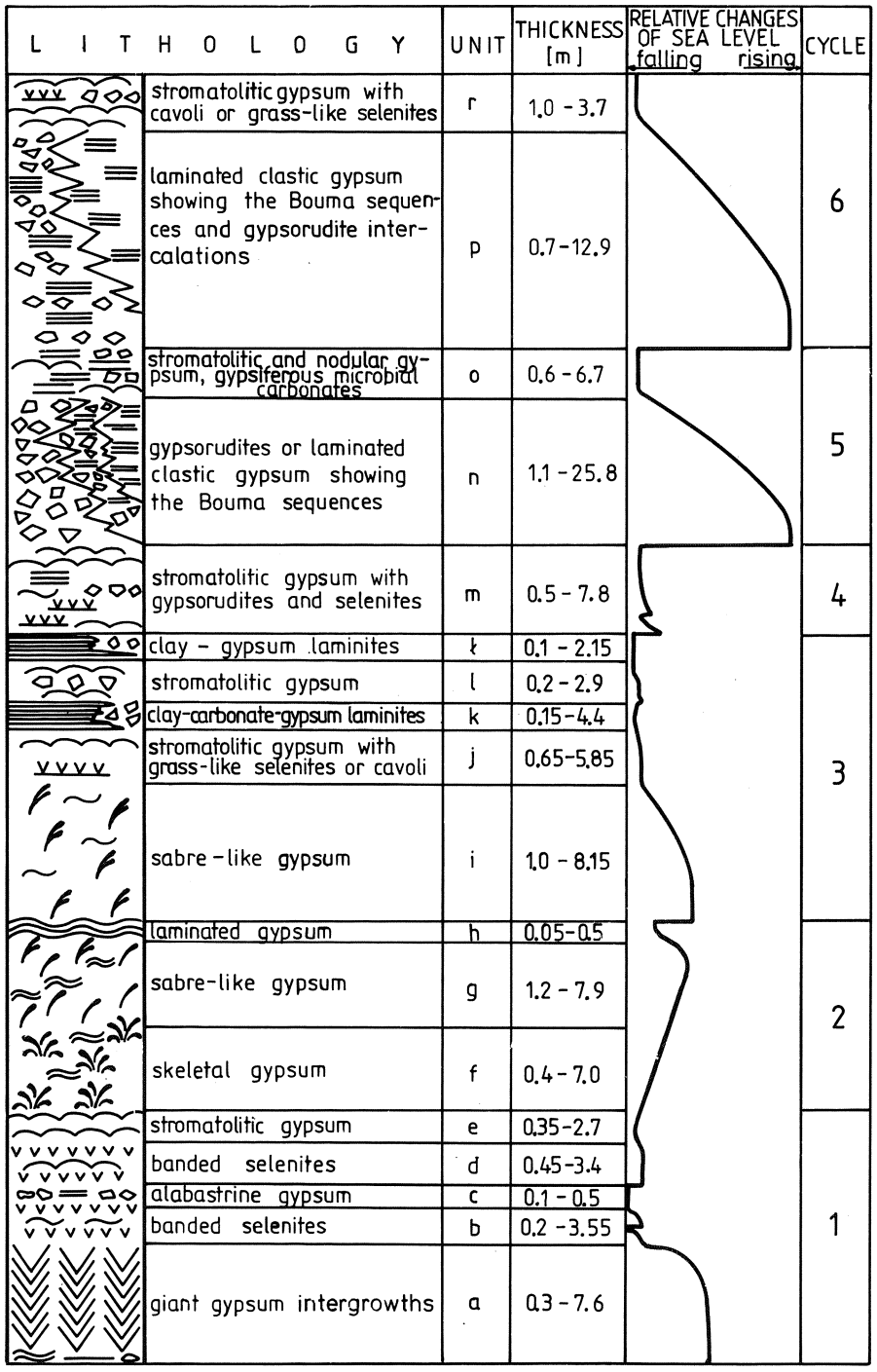

Fig. 7 Lithostratigraphical division of Miocene gypsum deposits south of the Góry Świętokrzyskie

the conditions of increasing salinity, as it was found by Orti Cabo *et al.* (1984) and Dronkert (1985) in the modern coastal salinas of southeast Spain. The common occurrence of gypsum-microbial laminites (biolaminites) typical of coastal sabkha (Kendall & Warren, 1988; Gunatilaka & Shearman, 1988), dome-like stromatolites formed in a rhythmically flooded and emergent environment, as well as selenite horizons growing in subaqueous conditions, indicates changing regimes of sedimentation during the deposition of units *b-e*. Similar lithofacies are known from extremely shallow-water to subaerial modern evaporite environments at the southeastern coasts of Spain (Orti Cabo *et al.*, 1984; Dronkert, 1985; author's own observations), southern and western Australia (Arakel, 1980; Warren, 1982; Logan, 1987) and the Persian Gulf (Purser *et al.*, 1987; Gunatilaka & Shearman, 1988).

The sea-level rise resulted in restoring the subaqueous conditions, though – as may be inferred from the morphology of the skeletal and sabre-like gypsum in units *f*, *g*, *i* – the depth of the sea was slightly less than that at which glassy gypsum had developed (Fig. 7). Spontaneous precipitation and crystal growth occurred at the bottom and near the water/air interface in the conditions of high salinity. The chaotical arrangement of selenite crystals in skeletal gypsum, intercalations of detritic gypsum, admixture of terrigenous material and deformational structures in laminated layers indicate elevated energy of environment.

Episodical lowering of sea level resulted in general predominance of physical accretion, recorded in the formation of a layer of laminated clastic sediment (unit *h* – Fig. 7). Characteristic sedimentary structures – graded bedding, ripples, cross-lamination and brecciation – prove mechanical remobilization and redeposition of clastic material by intermittent currents.

A renewed increase in depth and salinity permitted the continuation of the growth of sabre-like gypsum (unit *i* – Fig. 7). The appearance of laminae of peloidal limestone and brecciated horizons with selenite clasts in the upper part of the selenite complex indicates a distinct variation in the physico-chemical regime, which put end to the selenite growth in the most part of the area. This variation was probably caused by a distinct fall of sea level, increase in energy of environment and decrease in salinity, following a change of climate to a more humid one.

Evolution of sulphate sedimentation in the central part of the studied area was different (Fig. 5; Kasprzyk, 1991, fig. 8; Kasprzyk & Orti Cabo, in prep.). The drop in sea level at the end of the Baranów Beds deposition resulted in emergence of a large part of the central shoal. In its peripheral zone, the sequence of structures in the gypsum rocks (crystalline - stromatolitic - nodular) records a change of sedimentation from subaqueous to subaerial; typical sabkha sediments – nodular gypsum and anhydrite (Pl. IX: 2; Fig. 5) were laid down in the coastal zone at this time (Kasprzyk, 1991 – figs. 3, 4, 8). Episodic return to subaqueous conditions was marked by the development of selenite gypsum (Fig. 5), followed by another sea-level fall.

The fall of sea-level preceded essential changes in the physiographic system, which caused that the farther sedimentation in the central part of the studied area – hitherto slightly different in evolution – was similar as in the other areas.

The peripheral part of the basin and some parts of the shoals were emerged and extremely shallow water conditions reigned over the remaining area. Such a change in the sedimentary environment favoured the development of microbial facies, periodically interrupted or slowed down in conditions of dominant physical accretion or chemical precipitation (units *j-m*; Fig. 7; Pl. VI: 2; Pl. VII: 3). Gypsooid sands were laid down in the littoral zone by strongly agitated water (Bąbel & Kasprzyk, 1990; Fig. 3), then transported towards the adjacent lagoon and deposited in the parts of the bay better protected from the wave action. The increased supply of terrigenous material, possibly related to the fluvial supply loaded with the residuum after dissolution of the gypsum rocks, occurred mainly in the peripheral part of the basin. Modern facies analogs are the coastal salinas of western Australia (Logan, 1987) where strongly reworked clastic gypsum sediment is laid down in conditions of seasonally varying salinity and water agitation.

Mechanical remobilization and redeposition of gypsum sediments was conspicuous in the remaining area in the same time. Numerous synsedimentary structures in thick beds of clastic gypsum in the western part of the studied area (Fig. 2) point to a high degree of tectonic instability, interpreted as a trigger for the redistribution process (Peryt & Kasprzyk, 1992).

The rise in sea level resulted in restitution of subaqueous conditions in the whole studied area. It was in a close relation to the tectonic activity in the area of the Góry Świętokrzyskie which changed the morpho-structural pattern in the southern margin. This preceded an important change in the facies evolution.

Tectonic activity, probably accompanied by volcanic activity (proven by tuffite and tuffitic clay intercalations – Fig. 3-6), initiated redistribution of gypsum sediment by mass movements – debris flows, slumps and turbidity currents (unit *n* – Fig. 7; Kasprzyk, 1991, fig. 8; Peryt & Kasprzyk, 1992).

The sea level fall resulted in emergence of the peripheral part of the basin (Kasprzyk, 1991, fig. 6). Perhaps deposition continued there in an extremely shallow-water environment, and a later denudation resulted in the complete removal of sediments. This may be indicated by clasts of stromatolite gypsum and microbial-peloidal limestones in gypsorudites in the northern part of the studied area. Conditions favourable for the development of microbial and nodular facies (unit *o*: Fig. 7; Pl. VI: 1) prevailed in the remaining area. These are known from the modern sabkhas at the coasts of the Persian Gulf and the Mediterranean Sea (Kendall & Warren, 1988).

The tectonic rearrangement resulted in a new palaeogeographical pattern in the peripheral part of the evaporite basin (Kasprzyk, 1991, figs. 7, 8). The structural evolution was manifested in the eastward shift of the basin axis

which resulted in the intense redistribution of clastic material from the peripheral areas of the basin (unit *p*; Fig. 7).

Towards the end of the sulphate deposition the sea-level fell again (Fig. 7). The marginal zone was emerged and subject to intense denudation. Only locally microbial carbonates were laid down in extremely shallow hypersaline basins (ponds) of the coastal plain. The microbial mats were being gypsified in the conditions of elevated salinity, as was found in the Osiek area (Pl. VI: 3, 4). Horizons of finer selenite developed sporadically. Exteremely shallow-water to subaerial conditions, similar to those occurring now in ephemeral coastal lagoons in western Australia (Logan, 1987), prevailed in the northern marginal zone of the evaporite basin at the final stage.

Lithofacies of the sulphate deposits in the northern part of the Carpathian Foredeep indicate a large variation within the sedimentary environment (Fig. 8). The results of sedimentary processes, normally well marked in the lithology and in the assemblage of sedimentary structures, were partly or completely obliterated during diagenesis. The diagenetic modification included (Fig. 8): 1) dehydration (partial or complete replacement of gypsum by anhydrite), 2) hydration or rehydration (replacement of anhydrite by secondary gypsum), 3) bacterial reduction of sulphates (replacement of sulphates by carbonates with concentrations of native sulphur).

Causes of facies changes

The evolution of sulphate sedimentation was controlled mainly by tectonic and climatic factors (e.g. Pawłowski, 1970; Kwiatkowski, 1972; Garlicki, 1979; Kubica, 1985, 1992). The deposition of sulphate sediments occurred during sea-level fluctuations, small but well marked in rock record, which could be due to: 1) subsidence, 2) tectonic movements and (or) eustatic changes, and 3) evaporative drawdown. The presented reconstruction of the sedimentary history of the sulphate deposits stresses mainly the influence of tectonic and (or) eustatic changes which controlled the nature and sequence of sediments (Fig. 7). A detailed lithofacies analysis and correlation of the successions of established processes prove that the axis of evaporite basin migrated eastwards in the studied area during the deposition of the sulphate sediments (cf. Kasprzyk, 1991, fig. 8). This is in agreement with the earlier conclusions on the tectonic evolution of the Miocene basin (e.g. Ney *et al.*, 1974; Garlicki, 1979; Wilczyński, 1984).

Though the details of the succession of events in this area are still under debate (Ney *et al.*, 197; Oszczypko & Tomaś, 1985; Żytko, 1985), it is generally accepted that the salinary crisis in the Badenian basin was a result of diastrophic events related to the thrusting of the Carpathians from the south, and of the tectonic activity in their foreland.

The analysis of the complete sequences of lithofacies indicates that the sea level was falling five times (Fig. 7). In contrary to the first four sea-level falls

Table 3

Comparison of cyclical sequence of lithofacies in the Badenian gypsum south of the Góry Świętokrzyskie and in the Messinian of the Mediterranean area

	Carpathian Foredeep		Sicily, Ciminna Basin (Messinian)	Northern Apennines (Messinian)	SE Spain, Sorbas Basin (Messinian)
Number of cycles	6 1-4	5-6	4 or 5	13 or 14	12
Sequence of lithofacies in cycle					7. carbonate-silty-clayey laminites
			6. chaotic gypsum conglomerates	6. chaotic gypsum	6. curved selenitic twins, distorted gypsum aggregates ("supercones")
			5. wavy, needle-like selenite layers	5. nodular and lenticular selenite	5. massive selenite layers, selenite clasts
	4. stromatolitic gypsum, nodular gypsum, laminated gypsum, clay		4. bedded selenite	4. banded selenite	4. giant selenite crystals in vertical "tree-like" columns
	3. banded gypsum with selenitic horizons, stromatolitic and alabastrine gypsum	1. stromatolitic gypsum, nodular gypsum	3. massive selenite aith algal filaments	3. massive selenite	3. subhorizontal prismatic gypsum crystals
	2. selenitic gypsum (glassy, sabre-like, skeletal)	2. banded gypsum with selenitic horizons	2. algal carbonates	2. stromatolitic limestones, stromatolitic selenite, limestone breccias, laminated calcite-gypsum sandstones	2. "nucleation cones", pelitic laminites
	1. biolaminites, dark gypsiferous clays	1. clastic gypsum (gypsorudites, laminated gypsarenites and gypsopelites)	1. bituminous clays	1. bituminous shales	1. gypsum-carbonate-clay laminites
references	this paper		Lo Cicero & Catalano, 1976	Vai & Ricci Lucchi, 1976; Dronkert, 1985	Dronkert, 1976, 1985

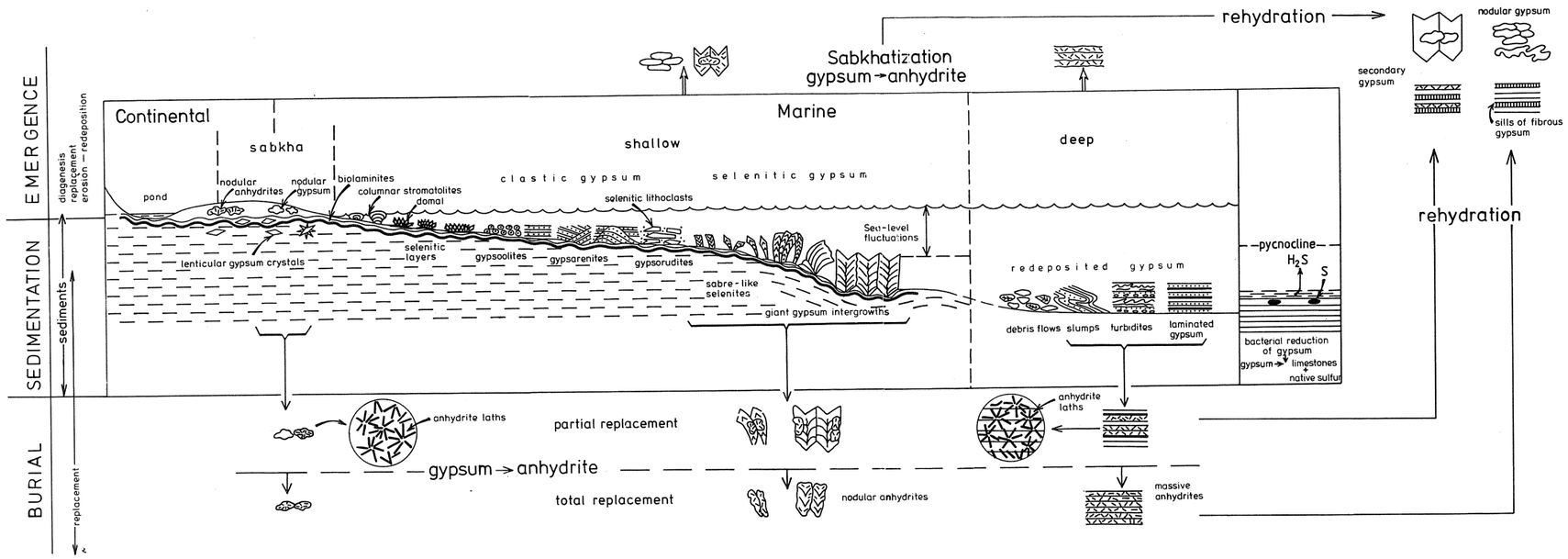

Fig. 8 Depositional environments and the extent of diagenetical transformation of gypsum sediment

which resulted only locally in episodic subaerial exposition of the area, after the fifth one the sea dried out nearly completely in the peripheral zone of the evaporite basin (Kasprzyk, 1991, figs. 7 and 8). In consequence, the nature of the deposition of sulphate deposits in the northern marginal zone of the evaporite basin may be described as regressive. The sea-level fluctuations were accompanied by variation in water salinity. These phenomena were the main causes of the cyclicity in the deposition of the sulphate sediments in the Carpathian Foredeep.

Cyclicity of sedimentation

Cyclic sedimentation is characteristic of evaporites (Sonnenfeld, 1984; Kendall, 1988). Cyclicity of sedimentation in the Messinian formation of the Mediterranean area is expressed in the repetitive lithofacies sequence (Table 3). There have been various opinions on the cyclicity in sulphate sediments in the Miocene of the Carpathian Foredeep. Most authors (e.g. Poborski, 1952; Niemczyk, 1961; Gaweł, 1962; Wala, 1962; Garlicki, 1968, 1979; Słomka, 1979; Kubica, 1985, 1992) accepted its existence though the opinions differed on the criterion of cyclicity and the number of sedimentary cycles (see discussion in Kubica, 1985). Cyclic nature of the Miocene gypsum was questioned by Kwiatkowski (1972).

The reconstruction of gypsum sedimentation presented in the preceding chapters allows for a distinction of six cycles (Fig. 7), well marked in a large part of the studied area. The successive stages of cyclic sedimentation, expressed by the repetitive lithofacies sequences (Table 3), record: 1) intensity and mutual relation between the processes of chemical precipitation, physical accretion and biological productivity, 2) regressive nature of deposition, 3) variable rate of sedimentation and subsidence. The regressive nature of depositional cycles is expressed in alternate occurrence of relatively deep-water and shallow-water facies (Fig. 7). The changes in depth caused by external factors (tectonic and (or) eustatic), subsidence, evaporation or sediment accumulation are clearly marked in the rock record (Figs. 2-6).

CONCLUSIONS

The rich assemblage of sedimentary structures in the Badenian sulphate sediments in the northern part of the Carpathian Foredeep indicates a significant variation in sedimentary environment in the peripheral zone of the evaporite basin. These environments, reconstructed on the base of analogy to the well studied facies of modern and fossil evaporite environments, represent both subaqueous (deep-water to extremely shallow-water) and subaerial environments (Figs. 7 and 8).

The marginal zone of the basin and the areas of shoals were emergent several times during the sulphate sedimentation (Fig. 7). The sea-level fall

preceded the development of sabkha sequence with the distinctive assemblage of sedimentary structures: cyanobacterial laminites, nodular and enterolithic structures, erosional structures and dessication-cracks (Table 2). Stromatolites, locally with selenite horizons (Fig. 8), were formed in extremely shallow-water to subaerial environments subject to frequent changes of the physico-chemical regime. Selenite developed in a high-salinity subaqueous environment, as a result of rapid precipitation and crystal growth on the bottom. The selenite crystals were eroded and partly dissolved in periods of increased water dynamics. Clastic gypsum sediment, remobilized and redeposited in shallow-water conditions, reveals characteristic sedimentary structures: cross-lamination, ripples and graded bedding. Periodical instability (see Peryt & Kasprzyk, 1992) triggered gravity-controlled mass and turbidity flows, which resulted in redistribution of clastic gypsum sediment from the marginal to the deeper parts of the basin.

A similar sedimentary evolution – from deep-water to subaerial facies – has been recognized in many ancient evaporite formations (see discussion in: Schreiber, 1986, 1988 and Warren, 1989, 1991). Among these, only the Messinian formation of the Mediterranean area includes perfectly preserved primary sulphate lithofacies, very similar to those in the Badenian sulphate sediments of the Carpathian Foredeep.

The development of evaporites in the Badenian basin was initiated by climatic and tectonic factors which controlled the major changes of the physico-chemical regime and the cyclic nature of sedimentation (Table 3). The repetitive lithofacies sequences record the intensity of the processes of crystallization, sedimentation, subsidence (both regional and local), and eustatic and (or) tectonic sea-level changes. The author distinguished six cycles in the gypsum sequence, marked in the repetitive sequence of relatively deep-water and shallow-water facies (Fig. 7). The sequence as a whole is regressive and – in analogy to the Messinian basins of the Mediterranean area – the evolution of the sulphate sedimentation records successive restriction of the evaporite basin down to complete emergence of its peripheral part.

Evaporite sediments are highly susceptible to diagenetic processes, resulting in partial or complete obliteration of the original structures of the rocks (Fig. 8). These processes were especially strongly manifested in the Badenian of the Carpathian Foredeep. Gypsum is replaced by anhydrite towards the deeper part of the foredeep, due to burial-related dehydration (Kubica, 1972, 1992). Anhydrite shows primary structures of gypsum rocks, often perfectly pre- served. In the conditions of increased migration of meteoric waters, initiated by tectonic modifications and (or) local exhumation, anhydrites were partly or completely hydrated and replaced by secondary gypsum.

Deep-water facies in the Badenian evaporite formation of the Carpathian Foredeep are represented by rock salt, sulphate basinal laminites and redeposited clastic sediments – turbidites, debris flows or submarine slumps; these are genetically related to morpho-structural depressions in the basin substrate

(Garlicki, 1979). The deep-water sediments are interstratified with or laterally replaced by shallow-water to subaerial sediments among which selenite lithofacies dominate.

ACKNOWLEDGEMENTS

This paper presents the main results of the Ph. D. thesis prepared in Państwowy Instytut Geologiczny under the supervision of Professor Tadeusz Peryt to whom I express my gratitude for the guidance and helpful remarks.

Many useful information and inspiring comments came from the discussions with Maciej Bąbel, Grzegorz Czapowski, Walter Dean, Andrzej Gąsiewicz, Axel Herrmann, Federico Orti Cabo, Josef Paul, Catherine Pierre, Juan Jose Pueyo Mur, Bruce Purser, Matthias Reimann, Laura Rosell-Ortiz, Jean-Marie Rouchy, Peter Scholle, Conchita Taberner. I wish to thank them all.

I extend my cordial thanks to Professor Aleksander Garlicki for his help and comments and to Docent Zbigniew Kowalczewski and Docent Zbigniew Rubinowski for enabling me this study and for their helpful comments and advice. I thank also Teresa Moszczyńska and Anna Stec for making the drawings, and Mrss. Janina Modrzejewska, Romana Ufnal and Alicja Walińska – for making the photographs.

REFERENCES

Arakel, A. V., 1980. Genesis and diagenesis of Holocene evaporitic sediments in Hutt and Leeman lagoons, Western Australia. *J. Sedim. Petrol.*, 50: 1305 – 1326.

Bąbel, M., 1984. Uwagi na temat budowy i rozwoju gipsów szklicowych. *Prz. Geol.*, 32: 577 – 582.

Bąbel, M., 1986. Growth of crystals and sedimentary structures in the sabre-like gypsum (Miocene, southern Poland). *Prz. Geol.*, 34: 204 – 208.

Bąbel, M., 1987. Giant gypsum intergrowth from the Middle Miocene evaporites of southern Poland. *Acta Geol. Polon.*, 37: 1 – 20.

Bąbel, M. & Kasprzyk, A., 1990. Gypsum ooids from the Middle Miocene (Badenian) evaporites of Poland. *Acta Geol. Polon.*, 40 (3-4).

Bellanca, A. & Neri, R., 1986. Evaporite carbonate cycles of the Messinian, Sicily: stable isotopes, mineralogy, textural features and environmental implications. *J. Sed. Petrol.*, 56 (5): 614 – 621.

Busquets, F., Orti, F., Pueyo, J. J., Riba, O., Rosell, L., Saez, A., Salas, R. & Taberner, C., 1985. Evaporite deposition and diagenesis in the Saline (Potash) Catalan Basin, Upper Eocene. In: Mils, M. D. & Rosell, J. (eds), *6th European Regional Meeting of Sedimentology, I.A.S., Lleida, Spain, Excursion Guidebook*, pp. 11 – 59.

Butler, G. P., 1970. Strontium geochemistry of modern and ancient calcium sulphate minerals. In: Purser, B. H. (ed.), *The Persian Gulf*. Springer-Verlag, New York, pp. 423 – 452.

Catalano, R., Renda, P. & Ślączka, A., 1976. Redeposited gypsum in the evaporitic sequence of the Ciminna Basin (Sicily). *Mem. Soc. Geol. It.*, 16: 83 – 93.

Ciarapica, G., Passeri, L. & Schreiber, C. B., 1985. Una proposta di classificazione delle evaporiti solfatiche. *Geologica Romana*, 24: 219 – 232.

Cody, R. D., 1976. Growth and early diagenetic changes in artificial gypsum crystals grown with bentonite muds and gels. *Geol. Soc. Am. Bull.*, 87 (8): 1163 – 1168.

Dean, W. E. & Anderson, R. Y., 1978. Salinity cycles; evidence for subaqueous deposition of Castile Formation and lower part of Salado Formation, Delaware Basin, Texas and New Mexico. *Circ. N. M. State Bur. Mines Miner. Resour.*, 159: 15 – 20.

Dronkert, H., 1976. Late Miocene evaporites in the Sorbas Basin and adjoining areas. *Mem. Soc. Geol. It.*, 16: 341 – 361.

Dronkert, H., 1985. Evaporite models and sedimentology of Messinian and Recent evaporites. *GUA, Papers of Geology, Ser. 1*, 24, 283 pp.

Garlicki, A., 1968. Z rozważań sedymentologicznych nad profilem autochtonicznej formacji solonośnej okolicy Wieliczki i Bochni. *Rocz. Pol. Tow. Geol.*, 38: 219 – 223.

Garlicki, A., 1979. Sedymentacja soli mioceńskich w Polsce. *Pr. Geol. Komis. Nauk Geol. PAN Kraków*, 119: 66 pp.

Garrison, R. E., Schreiber, B. C., Bernouilli, D., Fabricius, F. H., Kidd, R. B. & Méliéres, F., 1978. Sedimentary petrology and structures of Messinian evaporitic sediments in the Mediterranean Sea, Leg 42 A, Deep Sea Drilling Project. In: Hsü, K. J. & Montadert, L. et al., *In. Rep. Deep Sea Drill. Proj.*, 42, part I, Washington, pp. 571 – 612.

Gaweł, A., 1962. Budowa geologiczna złoża solnego Wieliczki. *Prace IG*, 30: 305 – 332.

Gavish, E., 1980. Recent sabkhas marginal to the southern coast of Sinai, Red Sea. In: Nissenbaum, A., (ed.), *Hypersaline brines and evaporitic environments*. Elsevier, Amsterdam, p. 233 – 251.

Gąsiewicz, A., 1990. Rozwój sedymentacji cechsztyńskiego dolomitu płytowego (Ca3) w rejonie Zatoki Puckiej. *Prz. Geol.*, 38: 187 – 195.

Goto, M., 1968. Oriented growth of gypsum in the Marion Lake gypsum deposits, South Australia. *J. Fac. Sci. Hokkaido Univ., Ser. 4, Geol. Min.*, 14 (1): 85 – 88. Sapporo.

Gradziński, R., Kostecka, A., Radomski, A. & Unrug, R., 1986. *Zarys sedymentologii*. Wyd. Geol. Warszawa, 628 pp.

Gunatilaka, H. A. & Shearman, D. J., 1988. Gypsum-carbonate laminites in a recent sabkha, Kuwait. *Carbonates and Evaporites*, 3 (1): 67 – 73.

Handford, C. R., 1981. A process-sedimentary framework for characterizing recent and ancient sabhas. *Sedim. Geol.*, 30: 255-265.

Hardie, L. A. & Eugster, H. P., 1971. The depositional environment of marine evaporites: a case for shallow clastic accumulation. *Sedimentology*, 16: 187 – 220.

Kasprzyk, A., 1989a. Litologia osadów siarczanowych miocenu w rejonie staszowskim. *Kwart. Geol.*, 33: 241 – 268.

Kasprzyk, A., 1989b. Zawartość strontu w mioceńskich skałach gipsowych w rejonie staszowskim. *Prz. Geol.*, 37: 201 – 207.

Kasprzyk, A., 1991. Analiza litofacjalna utworów siarczanowych badenu południowego obrzeżenia Gór Świętokrzyskich. *Prz. Geol.*, 39.

Kasprzyk, A., 1993. Stromatolitic structures in the Badenian gypsum deposits of southern Poland. *N. Jb. Geol. Palaeont. Mh.*, 187: 375 – 395.

Kasprzyk, A. & Bąbel, M., 1986. Gypsum ooids from the Miocene deposits of the vicinity of Staszów. *Prz. Geol.*, 34: 208 – 210.

Kendall, A. C., 1988. Aspects of evaporite basin stratigraphy. In: Schreiber, B.C. (ed.), *Evaporites and hydrocarbons*, pp. 11 – 65.

Kendall, C. G. St. C & Warren, J. K., 1988. Peritidal evaporites and their sedimentary assemblages. In: Schreiber, B. C., (ed.), *Evaporites and hydrocarbons*, pp. 66 – 138.

Kubica, B., 1972. O procesie dehydratacji gipsów w zapadlisku przedkarpackim. *Prz. Geol.*, 20: 184 – 189.

Kubica, B., 1985. Osady chemiczne. In: Pawłowski, S., Pawłowska, K. & Kubica, B., Budowa geologiczna tarnobrzeskiego złoża siarki rodzimej. *Pr. Inst. Geol.*, 114: 1 – 109.

Kubica, B., 1992. Rozwój litofacjalny osadów chemicznych badenu w północnej części zapadliska przedkarpackiego. *Pr. Państw. Inst. Geol.*, 133: 1 – 60.

Kwiatkowski, S., 1972. Sedymentacja gipsów mioceńskich Polski południowej. *Pr. Muz. Ziemi*, 19: 3 – 94.

Kwiatkowski, S., 1974. Złoża gipsów mioceńskich Polski południowej. *Biul. Inst. Geol.*, 280: 299 – 336.

Levy, Y., 1977. Description and mode of formation of the supratidal evaporite facies in northern Sinai coastal plain. *J. Sedim. Petrol.*, 47: 463 – 474.

Lo Cicero, G. & Catalano, R., 1976. Facies and petrography of some Messinian evaporites of the Ciminna Basin, Sicily. *Mem. Soc. Geol. It.*, 16: 63 – 81.

Logan, B. W., 1987. The MacLeod Evaporite Basin. Western Australia. *Am. Assoc. Petrol. Geol., Mem.* 44, 1 – 140.

Maiklem, W. R., Bebout, D. G. & Glaister, R. P., 1969. Classification of anhydrite: a practical approach. *Bull. Can. Petrol. Geol.*, 17 (2): 194 – 233.

Meier, R., 1975. Zu Einigen Sedimentgefuegen der Werra-Sulfate am Osthang der Eichfeld-Schwelle. *Z. Geol. Wiss.*, 3 (10): 1333- 1347.

Ney, R., Burzewski, W., Bachleda, T., Górecki, W., Jakóbczak, K. & Słupczyński, K., 1974. Zarys paleogeografii i rozwoju litologiczno-facjalnego utworów miocenu zapadliska przedkarpackiego. *Pr. Geol.*, 82: 65 pp.

Niemczyk, J., 1961. Badania złóż gipsów mioceńskich w rejonie Rzeszowa. *Prz. Geol.*, 9: 460 – 462.

Niemczyk, J., 1988a. Gipsarenity w mioceńskiej serii ewaporatowej w rejonie Wiślicy. *Geol.*, 14 (3): 51 – 56.

Niemczyk, J., 1988b. Litostratygrafia gipsów mioceńskich pomiędzy Buskiem a Wiślicą. *Geol.*, 14 (3): 105 – 115.

Orti Cabo, F., 1977. Aproximacion al estudio petrografico de las microestructuras de las rocas de yeso secundario y a su origen. *Rev. Inst. Inv. Geol.*, 32: 87 – 152.

Orti Cabo, F. & Shearman, D. J., 1977. Estructuras y fábricas deposicionales en las evaporitas del Mioceno superior (Messiniense) de San Miguel de Salinas (Alicante, España). *Inst. Invest. Geolog.*, 32: 5 – 54.

Orti Cabo, F. & Rosell Ortiz, L., 1982. Fábricas cristalinas de la anhidrita nodular y laminada. *Acta Geol. Hispanica*, 16 (4): 235 – 255.

Orti Cabo, F., Pueyo Mur, J. J., Geisler-Cussey, D. & Dulau, N., 1984. Evaporitic sedimentation in the coastal salinas of Santa Pola (Alicante, Spain). *Rev. Inst. Inv. Geol.*, 38/39, pp. 169-220.

Oszczypko, N. & Tomaś, A., 1985. Tectonic evolution of marginal part of the Polish Flysch Carpathians in the Middle Miocene. *Kwart. Geol.*, 29: 109 – 128.

Pawłowska, K., 1962. O gipsach, siarce rodzimej i pogipsowych skałach świętokrzyskiego miocenu. *Kom. Geol. PAN, Księga pam. ku czci prof. J. Samsonowicza.* Warszawa, pp. 69 – 82.

Pawłowski, S., 1965. Zarys budowy geologicznej okolic Chmielnika-Tarnobrzega. In: *Przew. 38 Zjazdu PTG*, pp. 8 – 20.

Pawłowski, S., 1970. Geologia złóż siarki w Polsce. Geologia i surowce mineralne Polski. *Biul. Inst. Geol.*, 251, pp. 614 – 635.

Pawłowski, S., Pawłowska, K. & Kubica, B., 1985. Budowa geologiczna tarnobrzeskiego złoża siarki rodzimej. *Pr. Inst. Geol.*, 114, pp. 1 – 109.

Peryt, T. M. & Antonowicz, L., 1990. Facje i paleogeografia cechsztyńskiego anhydrytu dolnego (A1d) w Polsce: *Przeg. Geol.*, 38: 173 – 180.

Peryt, T. M. & Kasprzyk, A., 1992. Earthquake-induced resedimentation in the Badenian (middle Miocene) gypsum of southern Poland. Sedimentology, 39: 235 – 249.

Poborski, J., 1952. Złoże solne Bochni na tle geologicznym okolicy. *Biul. PIG*, 78.

Purser, B. H., 1985. Coastal evaporite systems. In: Friedman G. M. & Krumbein, W. E. (eds.), Hypersaline Ecosystems - The Gavish Sabkha. *Ecol. Stud.*, Springer, pp. 72 – 102.

Purser, B. H., Soliman, M. & M'Rabet, A., 1987. Carbonate, evaporite, siliciclastic transitions in Quaternary rift sediments of the northwestern Red Sea. *Sedimentary Geology*, 53: 247 – 267.

Read, J. F., 1985. Carbonate platform facies models. *Am. Assoc. Petrol. Geol. Bull.*, 69: 1 – 21.

Richter-Bernburg, G., 1973. Facies and paleogeography of the Messinian evaporites in Sicily. In: Drooger, C.W. (ed.), *The Messinian Events in the Mediterranean*, pp. 124 – 141.

Richter-Bernburg, G., 1985. Zechstein-Anhydrite. *Geol. Jb., R. A*, 85: 1 – 82.

Rouchy, J. M., 1982. La gènese des évaporites Messiniennes de Méditerrannée. *Mem. Mus. Natn. Hist. Nat., série C*, 295 pp.

Schlager, W. & Bolz, H., 1977. Clastic accumulation of sulfate evaporites in deep water. *J. Sedim. Petrol.*, 47: 600 – 609.

Schreiber, B. C., 1978. Environments of subaquenous gypsum deposition. In: Dean, W. E. & Schreiber, B. C. (eds.), *Marine evaporites. S.E.P.M. Short Course notes*, no. 4, pp. 43 – 73.

Schreiber, B. C., 1986. Arid Shorelines and Evaporites. In: Reading, H. (ed.). *Sedimentary Environments and Facies*, pp. 189 – 228.

Schreiber, B. C., 1988. Subaqueous evaporite deposition. In: Schreiber, B. C. (ed.), *Evaporites and Hydrocarbons*, pp. 182-255.

Schreiber, B. C. & Decima, A., 1976. Sedimentary facies produced under evaporitic environments: A review. *Mem. Soc. Geol. Ital.*, 16: 111 – 126.

Schreiber, B. C., Friedman, G. M., Decima, A. & Schreiber, E., 1976. Depositional environments of Upper Miocene (Messinian) evaporite deposits of the Sicilian Basin. *Sedimentology*, 23: 729 – 760.

Schreiber, B. C., Roth, M. S. & Helman,M. L., 1982. Recognition of primary facies characteristics of evaporites and the differential of these forms from diagenetic overprints. In: Handford, C. R., Loucks, G. R., Davies, G. R. (eds), *Depositional and Diagenetic Spectra of Evaporites. Soc. Econ. Paleont. Mineral Core Workshop*, 3: 1 – 32.

Słomka, T., 1979. Przejawy cykliczności w procesie sedymentacji mioceńskich gipsów laminowanych. *Zesz. Nauk. AGH, Geol. Kwart.*, 5 (4): 59 – 65.

Sonnenfeld, P., 1984. *Brines and evaporites*. Academic Press, Orlando, pp. 613.

Vai, G. B. & Ricci Lucchi, F., 1977. Algal crust, autochthonous and clastic gypsum in a cannibalistic evaporite basin: a case history from the Messinian of Northern Apennines. *Sedimentology*, 24: 211 – 244.

Wala, A., 1962. Korelacja litostratygraficzna serii gipsowej obszaru nadnidziańskiego. *Spraw. z Pos. Kom. Nauk. PAN Kraków.*, VII-XII, pp. 530 – 532.

Wala, A., 1974. Charakterystyka petrograficzna i korelacja litostratygraficzna mioceńskich warstw gipsowych w otworach wiertniczych w rejonie Winiar. In: Strych, M., Dokumentacja geologiczna złoża gipsów mioceńskich Winiary w kat. C. *Archiwum Przedsiębiorstwa Geolog., Kraków* (unpublished).

Wala, A., 1979. Badania litologiczne mioceńskich warstw gipsowych i ilastych z wierceń na obszarze Niecki Nidy. In: Miłkowski, R., Sprawozdanie z prac badawczych mioceńskiej serii gipsonośnej w obszarze Niecki Nidy. *Archiwum Przedsiębiorstwa Geolog., Kraków.* (unpublished)

Wala, A., 1980. Litostratygrafia gipsów nidziańskich (fm). Symp. nauk "Gipsy Niecki Nidziańskiej i ich znaczenie surowcowe", pp. 5 – 10.

Warren, J. K., 1982. The hydrological setting, occurrence and significance of gypsum in late Quaternary salt lakes in South Australia. *Sedimentology*, 29: 609 – 637.

Warren, J. K., 1983. On the significance of evaporite lamination. *6th Int. Symposium on Salt*, 1: 161 – 170.

Warren, J. K., 1989. *Evaporite sedimentology. Importance in Hydrocarbon Accumulation.* Prentice Hall, New Jersey, 285 pp.

Warren, J. K. & Kendall, C. G. St. C., 1985. Comparison of sequences formed in marine sabkha (subaerial) and saline (subaqueous) setting - Modern and ancient. *Am. Assoc. Petrol. Geol. Bull.*, 69: 1013- 1023.

West, I. M., Ali, Y. A. & Hilmy, M. E., 1979. Primary gypsum nodules in a modern sabhka on the Mediterranean coast of Egypt. *Geology*, 7: 354 – 358.

Wilczyński, M. S., 1984. Tektonika obszaru miedzy Chmielnikiem, Szydłowem i Wiślicą w świetle danych geologicznych w tym zdjęć radarowych i satelitarnych. *Archiwum PIG*, Warszawa, 94 pp. (unpublished).

Żytko, K., 1985. Some problems of a geodynamic model of the Northern Carpathians. *Kwart. Geol.*, 29: 85 – 108.

Streszczenie

LITOFACJE I SEDYMENTACJA OSADÓW SIARCZANOWYCH BADENU (ŚRODKOWY MIOCEN) W PÓŁNOCNEJ CZĘŚCI ZAPADLISKA PRZEDKARPACKIEGO

Alicja Kasprzyk

Abstract: Osady siarczanowe badenu są reprezentowane przez gipsy pierwotne: krystaliczne selenitowe, zbite, klastyczne, gipsy wtórne i anhydryty. Gipsy pierwotne wykazują duże zróżnicowanie litofacjalne oraz bogaty inwentarz struktur sedymentacyjnych. Wyniki analizy facjalnej oraz współczesne analogie wskazują, że utwory te rozwijały się w zmiennych warunkach sedymentacji – od subakwalnych (głęboko- i płytkowodnych) do subaeralnych, w salinach i na obszarach sebhy w strefie rampy platformowej, charakteryzującej się niewielkim nachyleniem (< 1°) i zróżnicowaną morfologią. Sekwencja litotypów – od *a* do *r* – wyróżnionych w profilach gipsów, ma chara- kter regresywny i obejmuje 6 cykli sedymentacyjnych.

WSTĘP

Przedmiotem analizy litofacjalnej są osady siarczanowe badenu na południe od Gór Świętokrzyskich (Fig. 1). Ze względu na rozmieszczenie odsłonięć i wierceń badania skoncentrowane były w czterech rejonach (Fig. 1): nadnidziańskim, staszowskim, osieckim oraz rzeki Wschodniej. Osady siarczanowe tego obszaru są reprezentowane przez gipsy pierwotne (krystaliczne selenitowe, zbite, klastyczne, Pl. I-VIII; IX: 1), gipsy wtórne (Pl. X: 2) i anhydryty (Pl. IX: 2). Uwzględniając zróżnicowanie litofacjalne gipsów wyróżniono szereg odmian (Fig. 2-6; Tab. 1). Gipsy krystaliczne selenitowe obejmują litofacje: szklicowe, szablaste, szkieletowe i warstwowane z poziomami selenitów. Następną grupę tworzą gipsy zbite: z agregatami krystalicznymi, stromatolitowe, laminowane, smugowane, alabastrowe i gruzłowe. Do gipsów klastycznych zaliczono: oolity gipsowe, gipsopelity, gipsarenity i gipsorudyty.

LITOFACJE GIPSOWE

Wśród gipsów selenitowych unikalne wykształcenie wykazują gipsy szklicowe (sz) (Pl. I-II). Budują je wielkie (do 3,5 m wys.), blokowe zrosty krystaliczne symetryczne i asymetryczne, o powierzchni zrostu pionowej lub pochylonej (Bąbel, 1987, 1990). Kryształy budujące skrzydła zrostu zachowują podstawowe prawidłowości wzrostu selenitów: rozszczepienia, zakrzywienia górnej powierzchni, strefowy przyrost postaci słupa (120) wyznaczony przez smugi i laminy mineralnych i organicznych inkluzji (agregaty iłu i kalcytu, włókna sinic). Podobne struktury występują w wielkokrystalicznych gipsach selenitowych współczesnych przybrzeżnych salin południowej Australii (Goto, 1968; Warren, 1982, 1983; Kendall & Warren, 1988).

Gipsy szablaste (sa) (Pl. III: 1-3) wyróżniają się obecnością kryształów szablastych, których charakterystycznymi cechami są: silne wydłużenie (15 - 90 cm), zakrzywienie górnej powierzchni, rozszczepienia, regularne strefy przyrostu. Kryształy szablaste są w skale rozmieszczone chaotycznie lub kierunkowo (Pl. III: 3); w kopułach gipsowych (Pl. III: 1, 2) wykazują orientację promienistą. W przestrzeni między kryształami szablastymi występują drobne kryształy selenitowe oraz matriks ilasto-węglanowo-gipsowy, lokalnie zanieczyszczony materią organiczną. Obserwowano przewarstwienia gipsów zbitych lub klastycznych, struktury obciążeniowe, ugięcia i zestromienia lamin nad kryształami selenitowymi oraz kryształy złamane. Gipsy selenitowe z kryształami szablastymi podobnymi do wyżej opisanych są znane ze współczesnych przybrzeżnych salin południowo-wschodniej Hiszpanii i południowej Australii (Warren, 1982; Orti Cabo *et al.*, 1984), gdzie tworzą kopulaste pokrywy selenitowe.

Gipsy szkieletowe (sk) są zbudowane z kryształów selenitowych, o długości do 15 cm, wzajemnie poprzerastanych i rozmieszczonych chaotycznie w obrębie węglanowo-pelityczno-gipsowego matriks (Pl. III: 4). Podobne agregaty kryształów wydłużonych i chaotycznie zorientowanych tworzą jądra kopuł gipsowych, powstających współcześnie w salinach przybrzeżnych (Warren, 1982; Orti Cabo *et al.*, 1984; Kendall & Warren, 1988).

Gipsy warstwowane z poziomami selenitowymi (sl) zawierają przewarstwienia gipsów zbitych lub klastycznych (Pl. IV). Kryształy selenitowe tworzą struktury palisadowe typu murawy (*grass-like*) lub formy kopułkowato-kalafiorowate o wykształceniu *cavoli*. Pozostałe charakterystyczne struktury sedymentacyjne to: kieszeniowe wypełnienia przestrzeni między wierzchołkami kryształów selenitowych przez materiał detrytyczny, struktury stromatolitowe, ślady rozpuszczania i (lub) erozji kryszatałów, struktury obciążeniowe, poziomy zbrekcjowań, szczeliny z wysychania. Litofacje gipsów selenitowych o podobnym wykształceniu i inwentarzu struktur sedymentacyjnych były opisywane ze współczesnych salin przybrzeżnych południowej i zachodniej Australii oraz południowo-wschodniej Hiszpanii (Arakel, 1980; Warren, 1982, 1983; Orti Cabo *et al.*, 1984; Dronkert, 1985; Logan, 1987).

Gipsy zbite z agregatami krystalicznymi (cl) to odmiana przejściowa między gipsami krystalicznymi selenitowymi i zbitymi, co wyraża się obecnością kryształów selenitowych, o długości do 25 cm, występujących w skupieniach lub pojedynczo w tle gipsu mikrokrystalicznego i (lub) ziarnistego, zanieczyszczonego materiałem pelityczno-węglanowym. Pospolite są: struktury obciążeniowe, laminacja nieregularna i smużysta.

Gipsy stromatolitowe (st) (Pl. IV: 1; Pl. V) występują w sekwencji litofacji w różnym położeniu (Fig. 2-6). Ich cechą jest obecność dobrze zachowanych struktur organogenicznych, których zróżnicowanie morfologiczne i mikrostrukturalne pozwala na wyróżnienie kilku odmian: stromatolitów, laminitów sinicowych i biolaminitów (Pl. V; omówienie: Kasprzyk, 1993).

Gipsy laminowane (la) są zróżnicowane pod względem wykształcenia i

genezy. Laminacja jest wyrażona naprzemianległym ułożeniem lamin gipsowych: jasnych, grubości 0,1 - 3,0 mm, nieznacznie zanieczyszczonych iłem i węglanami, oraz ciemnych, grubości 0,01 - 0,5 mm, rzadziej do 1 mm, z większą domieszką materiału węglanowo-pelitycznego. Pospolita jest laminacja: pozioma lub falista, soczewkowa, smużysta, krenulowana, konwolutna (Pl. VII: 2; Pl. IX: 3). Współczesne odpowiedniki facjalne tych utworów to laminowane osady gipsowe, tworzące się w przybrzeżnych salinach Hutt i Leeman na zachodnim wybrzeżu Australii w okresowo zmiennych warunkach zasolenia wód i dostawy materiału terygenicznego (Arakel, 1980).

Gipsy smugowane (fl) wykazują laminację niewyraźną, miejscami zatartą i poprzerywaną, wyrażoną obecnością nieregularnych smug, wyróżniających się w tle gipsu mikrokrystalicznego lub ziarnistego ciemniejszą barwą i większą domieszką materiału pelitycznego.

Gipsy alabastrowe (al) to makroskopowo skały skrytokrystaliczne zbite, barwy kremowej, jasnoszarej lub beżowej, o charakterystycznej laminacji krenulowanej (Pl. IV; Pl. VII: 1). Występują one zazwyczaj w cienkich warstwach o nieregularnej, gruzłowatej powierzchni stropowej, niekiedy pokrytej wiązkami drobnych kryształów selenitowych o wykształceniu *cavoli*. Podobne osady tworzą się współcześnie w przybrzeżnych salinach i obszarach sebhy (Warren, 1982, 1983; Purser *et al.*, 1987).

Gipsy gruzłowe (no) zawierają gruzły sferyczne i elipsoidalne, o średnicy od 1 do 12 cm, rozmieszczone w obrębie ilasto-węglanowego matriks pojedynczo, jako formy izolowane, lub w skupieniach i warstwach. Charakterystyczna jest struktura enterolityczna. Współczesne odpowiedniki facjalne są znane z obszarów sebhy Zatoki Perskiej, wybrzeży Australii i Morza Śródziemnego (West *et al.*, 1979; Gavish, 1980; Warren & Kendall, 1985; Kendall & Warren, 1988).

Gipsy klastyczne (Pl. VII-IX: 1) wykazują cechy strukturalne i teksturalne typowe dla terygenicznego osadu klastycznego. Cechy te są następujące: a) skład mineralny – duży udział (15 - 50 %) materiału terygenicznego (minerały ilaste, kwarc, łyszczyki, skalenie, litoklasty); b) szkielet ziarnowy – klasty kryształów gipsu, litoklasty skał gipsowych, węglanowych i ilastych, szczątki zwęglonych roślin, bioklasty makro- i mikrofauny, peloidy, ooidy; c) spoiwo – porowe, porowo-kontaktowe lub typu masy wypełniającej gipsowo-ilasto-węglanowe, gipsowo-margliste lub ilasto-margliste; d) struktury sedymentacyjne – struktura homogenicznie klastyczna, laminacja: równoległa pozioma lub falista, soczewkowa, smużysta i konwolutna, uziarnienie frakcjonalne, warstwowanie przekątne, riplemarki, sekwencje turbidytowe. Gipsy klastyczne obejmują odmiany: gipsoolity (oo), gipsopelity (gp), gipsarenity (ga) i gipsorudyty (gr), zróżnicowane pod względem wykształcenia i genezy. Współczesne odpowiedniki litofacji płytkowodnych są znane z przybrzeżnych salin i obszarów sebhy wybrzeży Australii, Hiszpanii, USA i Egiptu (Arakel, 1980; Warren, 1982; Orti Cabo *et al.*, 1984; Schreiber, 1986; Dronkert; 1985), gdzie silnie przerobiony klastyczny osad gipsowy tworzy się w okresach

zwiększonej agitacji wód.

INTERPRETACJA ŚRODOWISKA SEDYMENTACJI

Duże zróżnicowanie litofacjalne (Fig. 2-6) oraz bogaty inwentarz struktur sedymentacyjnych (Tab. 1) w osadach siarczanowych wskazuje na zmienne warunki sedymentacji w brzeżnej strefie badeńskiego basenu ewaporacyjnego. Warunki te, zrekonstruowane w oparciu o podobieństwo do dobrze poznanych – pod względem facjalnym – współczesnych i kopalnych środowisk ewaporacyjnych, reprezentują środowiska zarówno subakwalne (głębokowodne do skrajnie płytkowodnych), jak i subaeralne (Fig. 8).

W trakcie depozycji osadów siarczanowych w strefie peryferycznej zbiornika i na obszerze płycizn kilkakrotnie doszło do subaeralnych wynurzeń (Fig. 7). Obniżenie poziomu morza poprzedziło rozwój sekwencji sebhy z charakterystycznym zespołem struktur sedymentacyjnych: laminitami sinicowymi, strukturami gruzłowymi i enterolitycznymi, powierzchniami erozyjnymi i szczelinami z wysychania (Tab. 2). W środowiskach skrajnie płytkowodnych do subaeralnych, charakteryzujących się częstymi zmianami reżimu fizyko-chemicznego, rozwijały się utwory stromatolitowe, lokalnie z poziomami selenitowymi (Fig. 8). Gipsy selenitowe tworzyły się w środowisku subakwalnym o wysokim zasoleniu wód w efekcie szybkiego wytrącania i wzrostu kryształów na dnie. W okresach zwiększonej dynamiki wód lub wynurzenia kryształy selenitowe były erodowane i (lub) częściowo rozpuszczane. Klastyczny osad gipsowy, który był remobilizowany i redeponowany w warunkach płytkowodnych, wykazuje charakterystyczne dla środowiska płytkowodnego struktury sedymentacyjne: warstwowanie przekątne, riplemarki i uziarnienie frakcjonalne. Okresowa niestabilność uaktywniała grawitacyjnie warunkowane ruchy masowe o charakterze osuwiska, spływu rumoszowego lub prądu zawiesinowego, które powodowały redystrybucję klastycznego osadu gipsowego z obszarów płytkowodnych do głębszych części zbiornika.

Podobny do wyżej przedstawionego rozwój sedymentacji, charakteryzujący zróżnicowane środowiska depozycji – od głębokowodnych do subaeralnych – został rozpoznany w wielu kopalnych formacjach ewaporatowych (omówienie: Schreiber, 1986, 1988; Warren, 1989). Spośród nich jedynie formacja messyńska rejonu śródziemnomorskiego zawiera doskonale zachowane pierwotne litofacje siarczanowe, wykazujące duże podobieństwo do osadów siarczanowych badenu zapadliska przedkarpackiego.

Rozwój ewaporatów był zainicjowany czynnikami klimatycznymi i tektonicznymi, które determinowały zasadnicze zmiany reżimu fizyko-chemicznego oraz cykliczny charakter sedymentacji (Fig. 7, Tab. 3). Powtarzające się sekwencje litofacji rejestrują natężnie procesów: krystalizacji i (lub) sedymentacji, subsydencji – zarówno regionalnej, jak i lokalnej – oraz eustatyczno-tektonicznych wahań poziomu morza. W sekwencji gipsowej na połu-

dnie od Gór Świętokrzyskich autorka wydzieliła sześć cykli wyrażonych powtarzającym się następstwem facji względnie głębokowodnych i płytkowodnych (Fig. 7). Sekwencja ta, jako całość, ma charakter regresywny i – podobnie jak w basenach messyńskich rejonu śródziemnomorskiego – rozwój sedymentacji osadów siarczanowych rejestruje stopniowe ograniczenie zbiornika ewaporacyjnego aż do prawie całkowitego wynurzenia jego peryferycznej części.

Osady ewaporatowe są bardzo podatne na procesy diagenetyczne, prowadzące do częściowego lub całkowitego zatarcia pierwotnych struktur skał (Fig. 8). W badenie zapadliska przedkarpackiego procesy te zaznaczyły się szczególnie intensywnie. Ku środkowej części zapadliska przedkarpackiego gipsy są zastępowane anhydrytami w efekcie dehydratacji, związanej z pogrążeniem (Kubica, 1972, 1992). W anhydrytach są obserwowane – często doskonale zachowane – struktury pierwotnych skał gipsowych. W warunkach zwiększonej migracji wód meteorycznych, zainicjowanej tektoniczną przebudową i (lub) lokalnymi wynurzeniami, anhydryty uległy częściowej lub całkowitej hydratacji i zastąpieniu przez gips wtórny.

W badeńskiej formacji ewaporatowej zapadliska przedkarpackiego litofacje głębokowodne są reprezentowane przez sole kamienne, siarczanowe laminity basenowe oraz redeponowane osady klastyczne o cechach osadu turbidytowego, spływu rumoszowego lub osuwiska; genetycznie są one związane z obniżeniami morfo-strukturalnymi podłoża (Garlicki, 1979). Osady głębokowodne są przewarstwiane lub facjalnie zastępowane przez utwory płytkowodne do subaeralnych, wśród których dominują litofacje selenitowe. Podobny układ stosunków facjalnych, wyrażony następstwem facji od płytkowodnych w strefie platformowej przez osady redeponowane skłonu platformy do facji basenowych, rozwijających się w dystalnych partiach zbiornika, jest charakterystyczny dla wielu kopalnych głębokowodnych basenów ewaporatowych, np.: basenu cechsztyńskiego Europy środkowej (Schlager & Bolz, 1977; Richter-Bernburg, 1985; Peryt & Antonowicz, 1990), permskiego basenu Delaware w Teksasie (Anderson, 1982; Dean & Anderson, 1974; Dean, 1978a,b), messyńskich basenów Sycylii (Catalano *et al.*, 1976; Schreiber & Decima, 1976; Schreiber *et al.*, 1976) i północnych Apeninów (Vai & Ricci Lucchi, 1977; Dronkert, 1985) oraz eoceńskiego basenu Katalonii (Busquets *et al.*, 1984). Przedstawione w niniejszym opracowaniu wyniki badań litofacjalnych dostarczają nowych informacji o rozwoju sedymentacji osadów siarczanowych w strefie brzeżnej basenu ewaporatowego. Stosunki facjalne między peryferyczną a centralną częścią badeńskiego basenu zapadliska przedkarpackiego nie są jeszcze w szczegółach rozpoznane. Można przypuszczać, że ich wyjaśnienie umożliwi korelację osadów siarczanowych i chlorkowych, jak również pozwoli na przedstawienie szczegółowego modelu sedymentacji w mioceńskim basenie ewaporacyjnym przedpola Karpat.

EXPLANATIONS OF PLATES

Authors of photographs
Pl. I: 1; Pl. II: 1, 3; Pl. III: 1-3; Pl. IV: 1, 2 - T. Peryt
Pl. I: 2, 3; Pl. II: 2 - Z. Migaszewski
Pl. III: 4 - M. Skuza
Pl. V: 1; Pl. VI: 1; Pl. VII: 103; Pl. VIII: 1-3; Pl. IX: 1-3 - J. Modrzejewska & R. Ufnal
Pl. V: 2, 3; Pl. VI: 2-4; Pl. VIII: 4; Pl. X: 1, 2 - author

Plate I

Glassy gypsum; unit *a*

1 — Vertical or slightly inclined giant blocky crystalline intergrowths. Intergrowth planes (cs) with fan-like arrangement of crystals. Bogucice-Skalki.
2 — Irregular contact of glassy gypsum (a) with clayey-marly deposits of the substrate (B). Flat dissolution surface visible within the selenite layer (arrows). Gacki.
3 — Dissolution surface (black arrows) locally obliterated by syntaxial crystal growth (white arrow). Smaller intergrowths of second generation (a) are oriented perpendicular to the irregular dissolution surface. Marzęcin.

Plate II

Glassy gypsum; unit *a*

1 — Giant blocky crystalline intergrowths composed of split crystals, arranged symmetrically with respect to the vertical or slightly inclined intergrowth surface (= fracture surface, arrows) with distinct relief (cs). Chotel Czerwony.
2 — Asymmetrical, inclined crystalline intergrowth with a second generation of smaller intergrowths (arrows) in the upper, better grown flank. Chwałowice.
3 — Inclined crystalline intergrowths; in the middle part - asymmetrical intergrowth (a_1) with curved composition surface (underlined), in the upper part - chaotically arranged smaller intergrowths (arrows). Borków.

Plate III

Skeletal and sabre-like gypsum

1 — Gypsum dome with distinguishable central part (f) and outer, well stratified part (g) with radial arrangement of sabre-like crystals. Height of exposure 3.9 m. Wiślica.
2 — Close-up of dome from Pl. III: 1. The central part is built of skeletal gypsum with chaotically arranged crystals (unit *f*). Splitting (arrows) of strongly elongated (up to 70 cm), subhorizontally oriented sabre-like crystals. Bedding obliterated by syntaxial growth of crystals.
3 — Sabre-like gypsum with uniformly oriented, strongly elongated selenite crystals; space between them filled with chaotically oriented finer gypsum crystals. Unit *g*. Chwalowice.
4 — Skeletal gypsum with chaotically arranged selenite crystals and synsedimentary intercrystalline voids (black spots). Unit *f*. Borehole Zawada 1, depth 40.0 - 40.2 m.

Plate IV

1 — Lower part of gypsum sequence, composed of banded gypsum with selenite horizons (units *b* and *d*), alabastrine gypsum (unit *c*) and stromatolite gypsum (unit *e*). Note variation in thickness of unit *c*, controlled by dome-like arrangement of overlying selenite layers. Chotel Czerwony-Zagórze.
2 — Contact of units *b* and *c*. Close-up of the fragment marked in Pl. IV: 1. Chotel Czerwony-Zagórze.

Plate V

1 — Biolaminite with nodules and nodular laminae of lenticular gypsum. Gypsum-clayey-organic laminae distinctly deformed around the gypsum nodules. Base of gypsum sequence. Borehole Pocieszka 3, depth 63.25 m.
2 — Microscopic view of biolaminite from Pl. V: 1. Note uniform orientation of lenticular gypsum crystals. Crossed nicols.
3 — Gypsum-clayey-organic laminite at the base of gypsum sequence. Black laminae - clayey-organic, grey laminae - gypsum-clayey with chaotically distributed larger, lenticular gypsum crystals (white spots). Borehole Staszów 2, depth 51.35-51.40 m. Crossed nicols.

Plate VI

Cyanobacterial-peloidal gypsum limestones
1 — Irregular layers and clasts of cyanobacterial-peloidal gypsum limestones (pl) in brecciated stromatolitic gypsum with crystalline aggregates. Unit *o*. Borehole Lipnik 98, depth 140.5-140.62 m.
2 — Gypsum pseudomorphs after halite crystals (black arrows), peloids and organic laminae (white arrows) in gypsum-carbonate background. Unit *m*. Borehole Lipnik 98, depth 149.6 m. Crossed nicols.
3 — Horizontally elongated cyanobacterial filaments (black) and single peloids (arrows) in micritic gypsum-carbonate background; G - cluster of granular gypsum. Unit *r*. Borehole Lipnik 98, depth 124.1 m. Crossed nicols.
4 — Clasts of gypsiferous peloidal limestone (pl) in gypsum-marly matrix. Unit *r*. Borehole Lipnik 97, depth 146.2 m. Crossed nicols.

Plate VII

Laminated and clastic gypsum
1 — Erosional channel in clayey-gypsum rhythmite overlying irregular, nodular top of alabastrine gypsum (al). Deformed and fragmented gypsum laminae (arrows) in laminated package. The channel is filled with fragments of gypsum laminae and lithoclasts of pyrite-bearing claystone (black), chaotically distributed in gypsum-clayey matrix. Unit *c*. Borehole Suchowola 81, depth 89.35-89.50 m.
2 — Package of marly-gypsum (G) and marly-clayey (C) laminae, cross (herring-bone) stratified, covered with regularly horizontally laminated gypsum with microfaults (arrows). Unit *p*. Borehole Pliskowola 30, depth 108.5 m.
3 — Gypsum (light) and gypsum-marly (grey) laminae in sets of cross laminae. Unit *k*. Borehole Osiek 141, depth 84.7 m

Plate VIII

Gypsorudites and gypsarenites
1 — Gypsarenite (ga) flaser and lenticular laminated, with graded laminae and sharp contact with overlying gypsorudite (upper part). Note abraded clasts of graded gypsarenites (ga_1). Unit *p*. Borehole Lipnik 98, depth 133.85-134.0 m.
2 — Fragments of laminated and flaser gypsum in abundant gypsarenite matrix. Unit n. Borehole Przyborów 1, depth 256.8-257.0 m.
3 — Abraded and corroded clasts of selenite (white arrows), laminated gypsum (empty arrows) and gypsum-carbonate breccia (black arrows) in gypsarenite matrix. Unit *n*. Borehole Suchowola 80, depth 90.2-90.4 m.
4 — Microscopic view of gypsarenite matrix. Clasts of gypsum crystals (G), sometimes twinned (arrows), chaotically distributed in gypsum-clayey-carbonate matrix of background type. Unit *n*. Borehole Osiek 156, depth 84.4 m. Crossed nicols.

Plate IX

1 — Convolution in laminated clastic gypsum. Unit *n*. Borehole Pliskowola 77, depth 116.4 - 116.5 m.
2 — Anhydrite with chicken-wire texture. Irregular sulphate nodules, isolated or connected, in clayey-dolomitic matrix. Unit *b*. Borehole Strzelce 1, depth 394.5-394.6 m.
3 — Laminated gypsum with effects of dehydration and replacement by chaotically prismatic or radially fibrous anhydrite aggregates (arrows). Sample is cut by vein of granular and microcrystalline anhydrite with an aureole of anhydrite laths. Unit *n*. Borehole Strzelce 1, depth 382.2-382.35 m.

Plate X

1 — Chaotically prismatic and radial fibrous aggregates of anhydrite laths in microcrystalline gypsum background. Unit *i*. Borehole Okrągła 31-9, depth 280.3 m. Crossed nicols.
2 — Secondary gypsum with amoeboidal (porphyroblastic) microstructure. Unit *a*. Borehole Okrągła 31-9, depth 289.9 m. Crossed nicols.

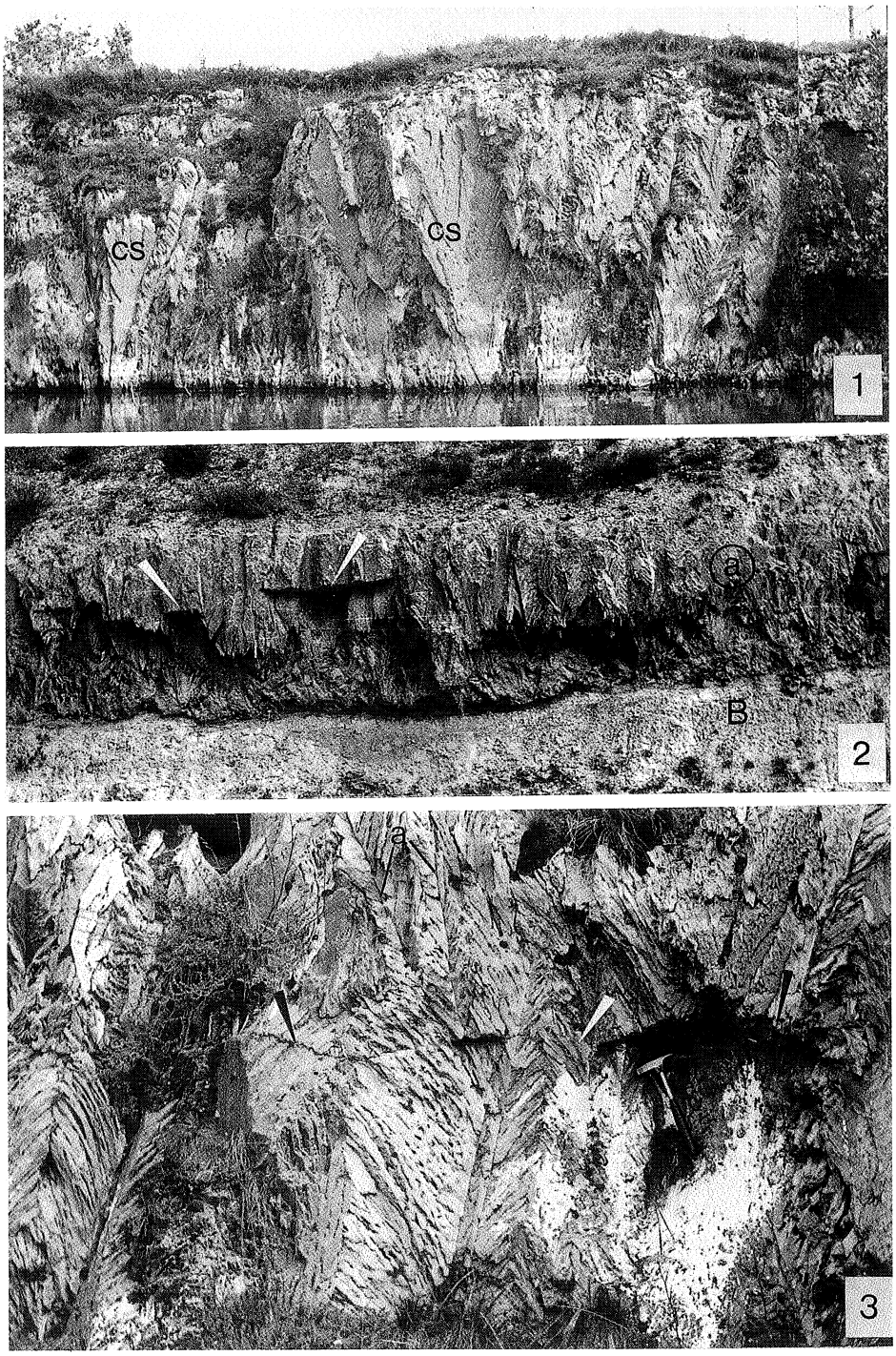
CS
CS
1
a
B
2
a
3


CS
1
2
a1
3

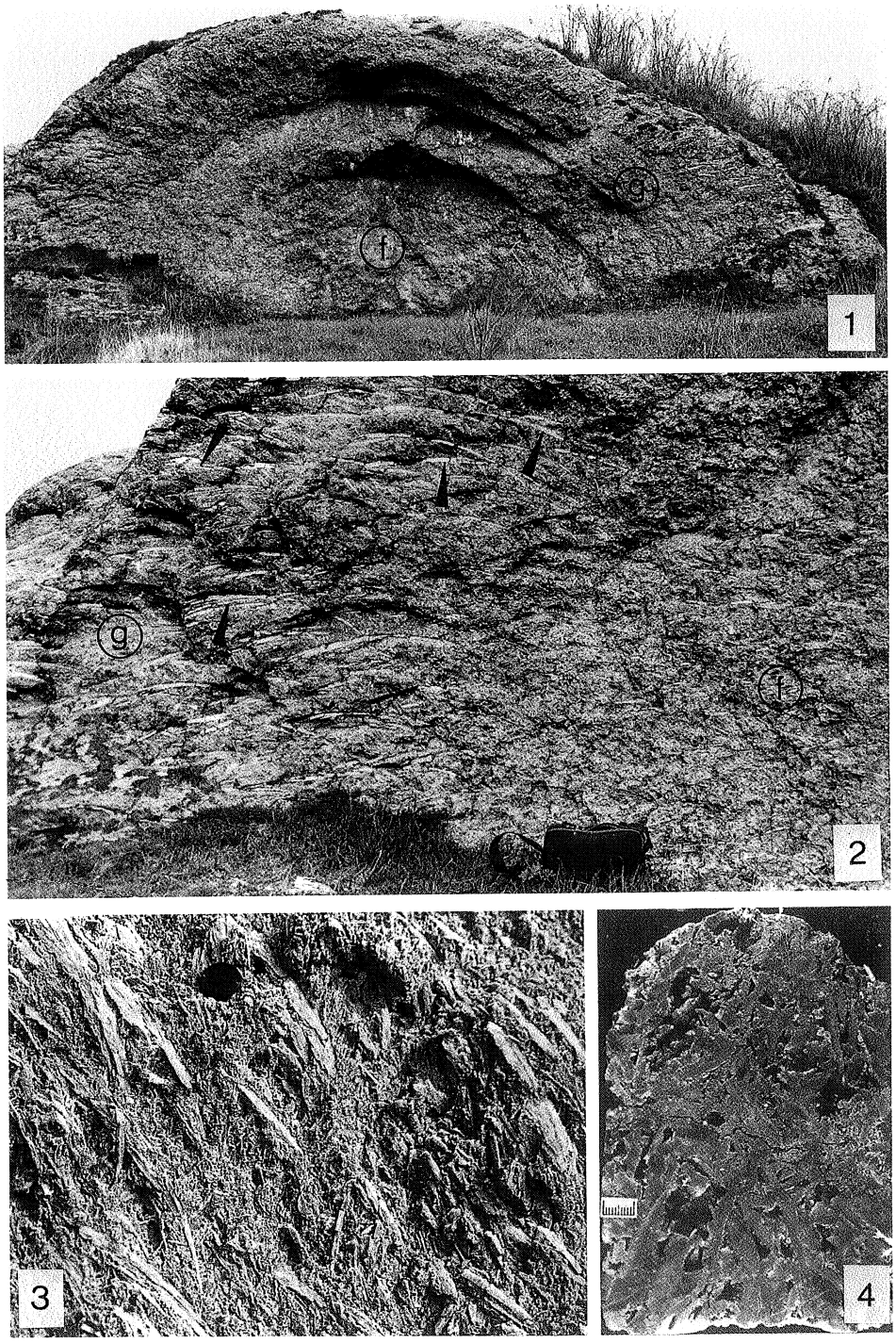
f
g
1
g
f
2
3
4


e
d
c
b
1

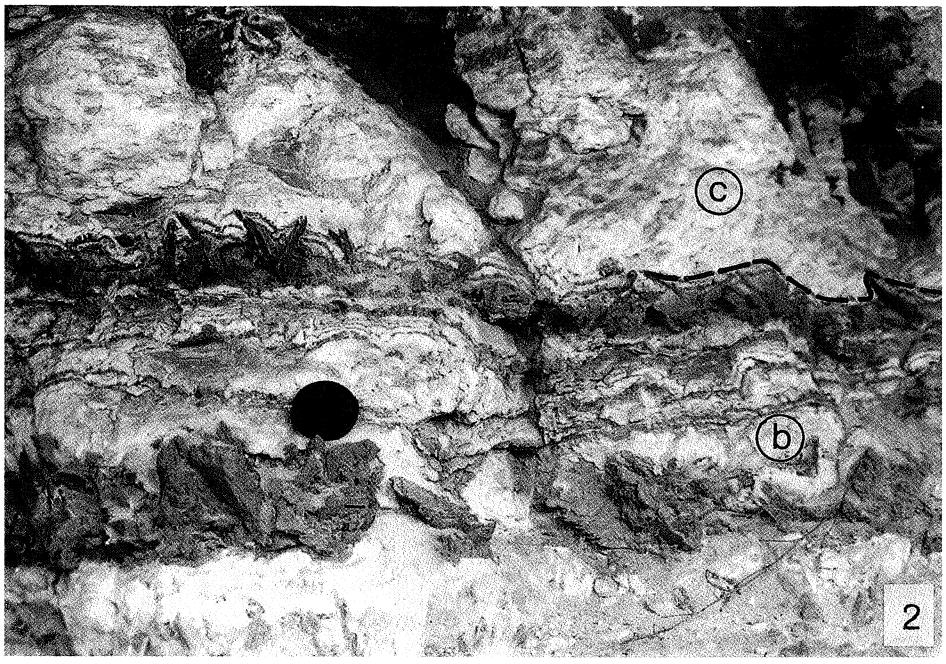
c
b
2

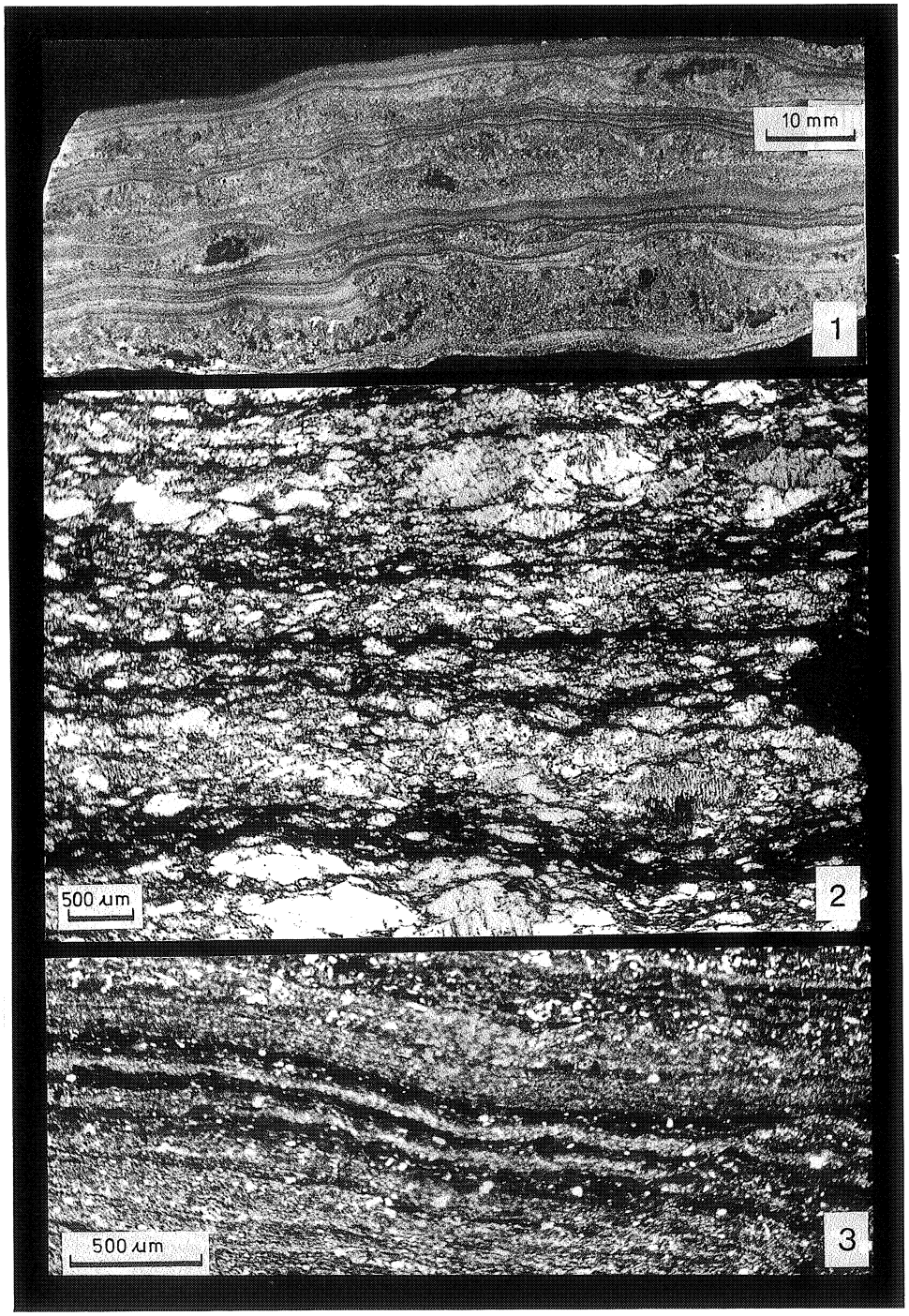
10 mm
1
500 µm
2
500 µm
3

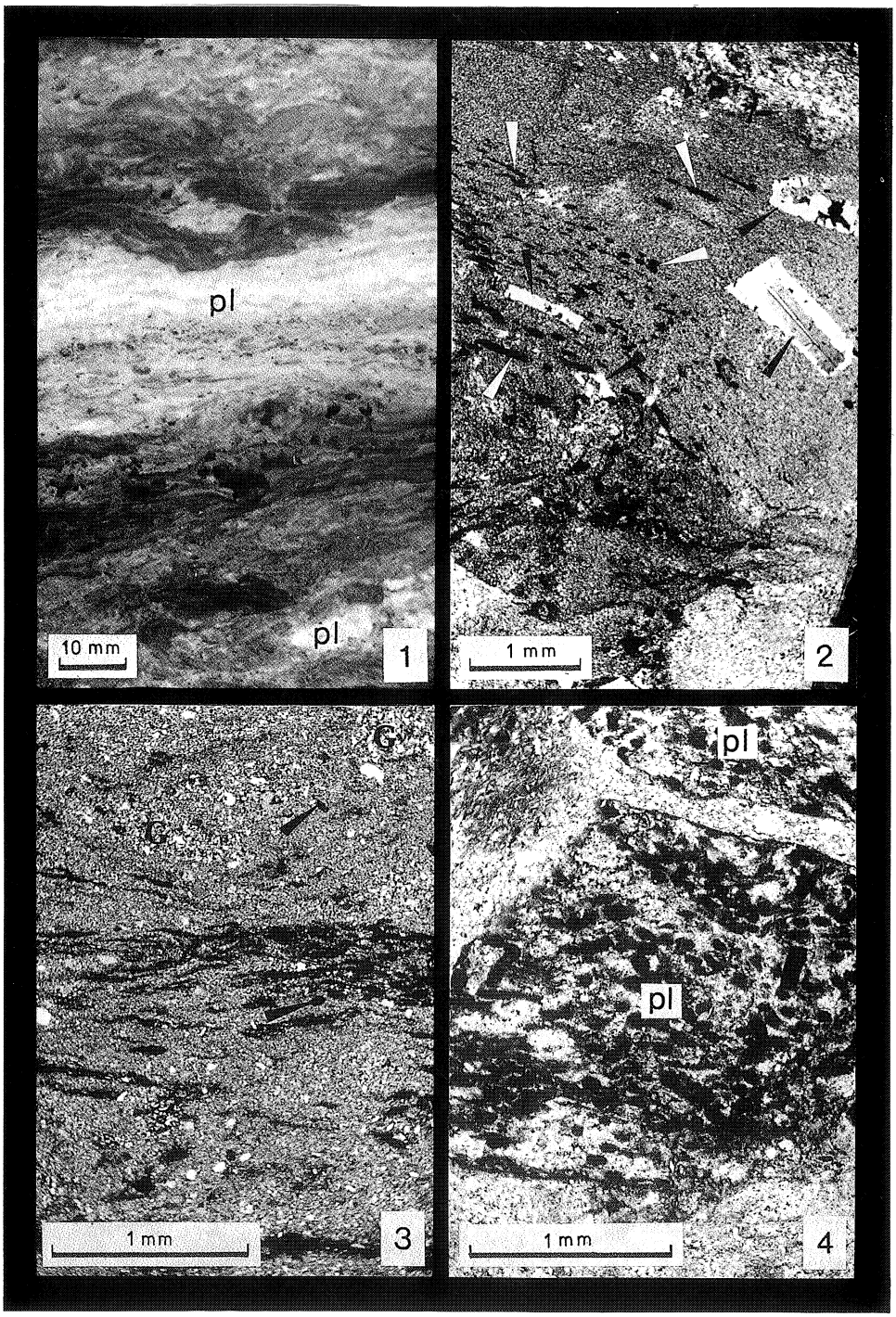
pl
pl
10 mm
1
1 mm
2
G
G
1 mm
3
pl
pl
1 mm
4

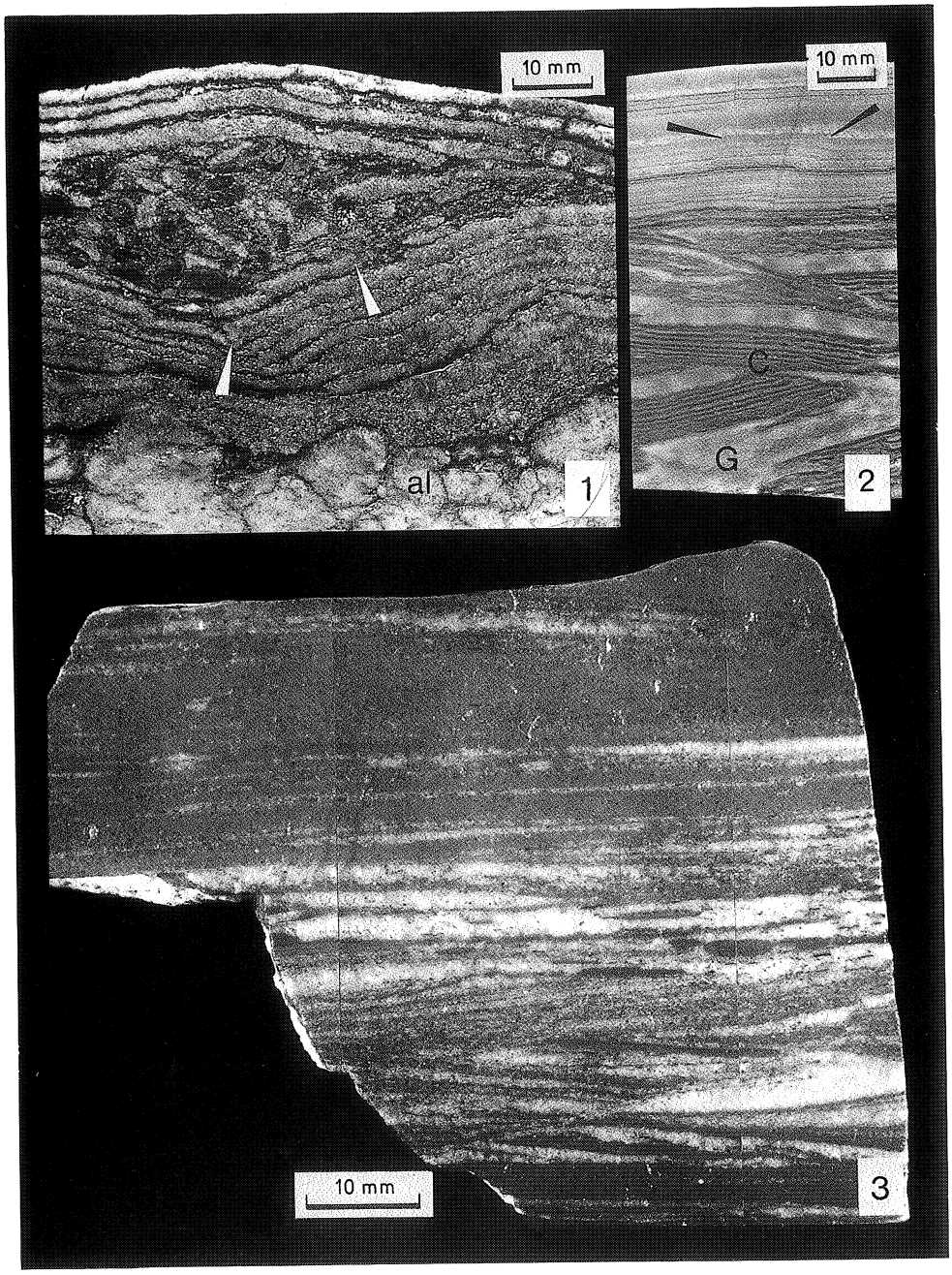
10 mm
al
1
10 mm
C
G
2
10 mm
3

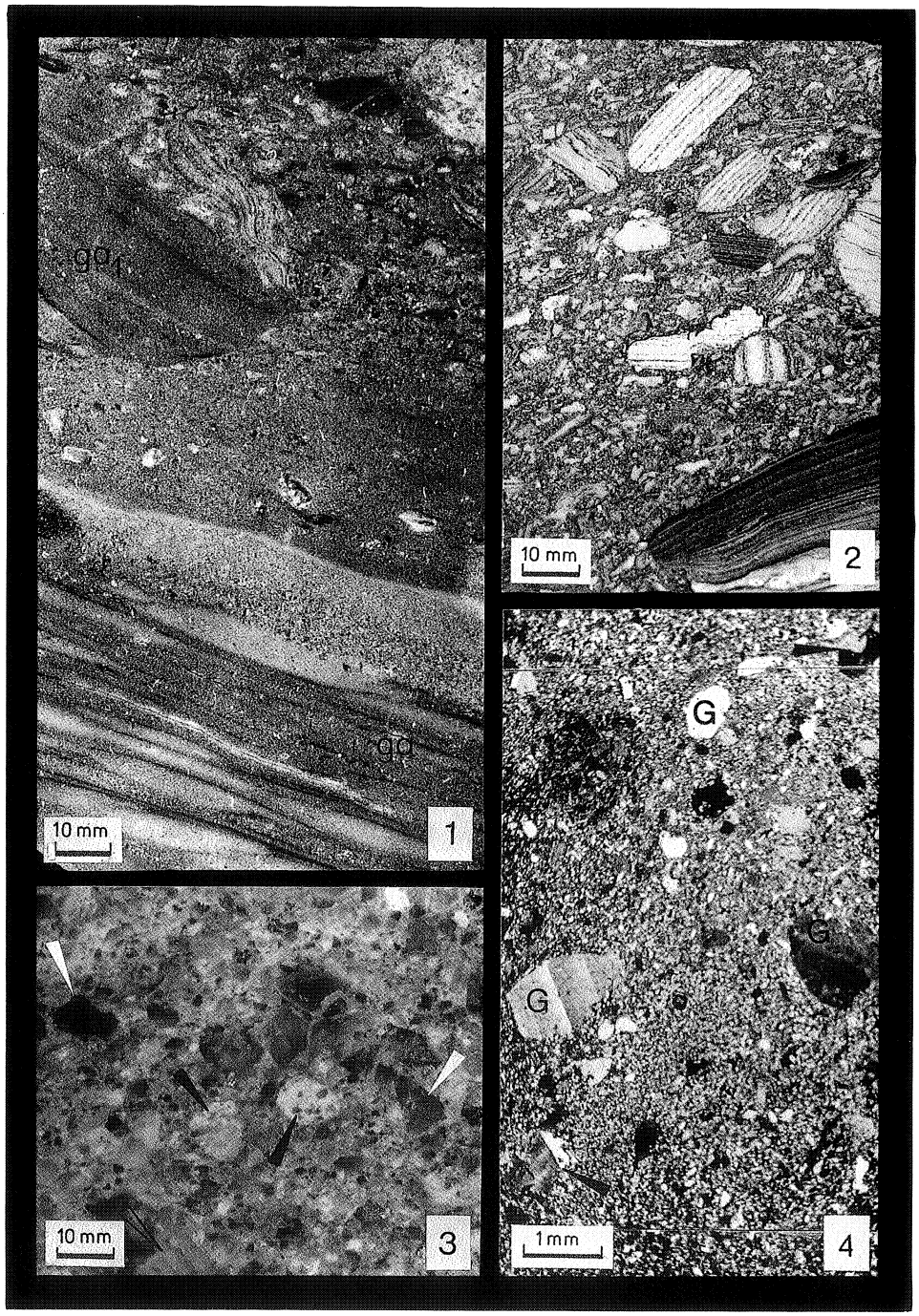
gg1
gg
10 mm
1
10 mm
2
10 mm
3
G
G
G
1 mm
4

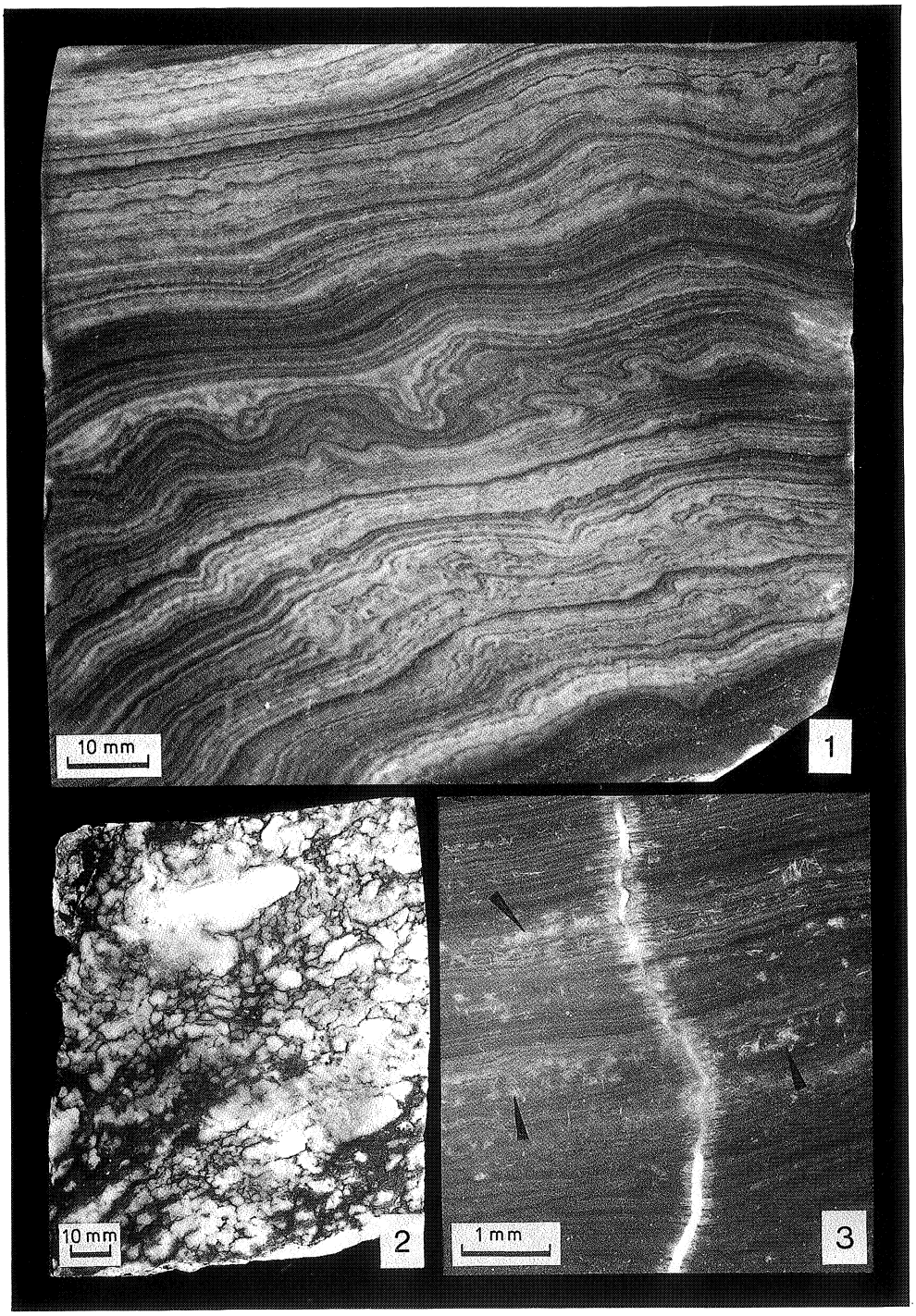
10 mm
1
10 mm
2
1 mm
3

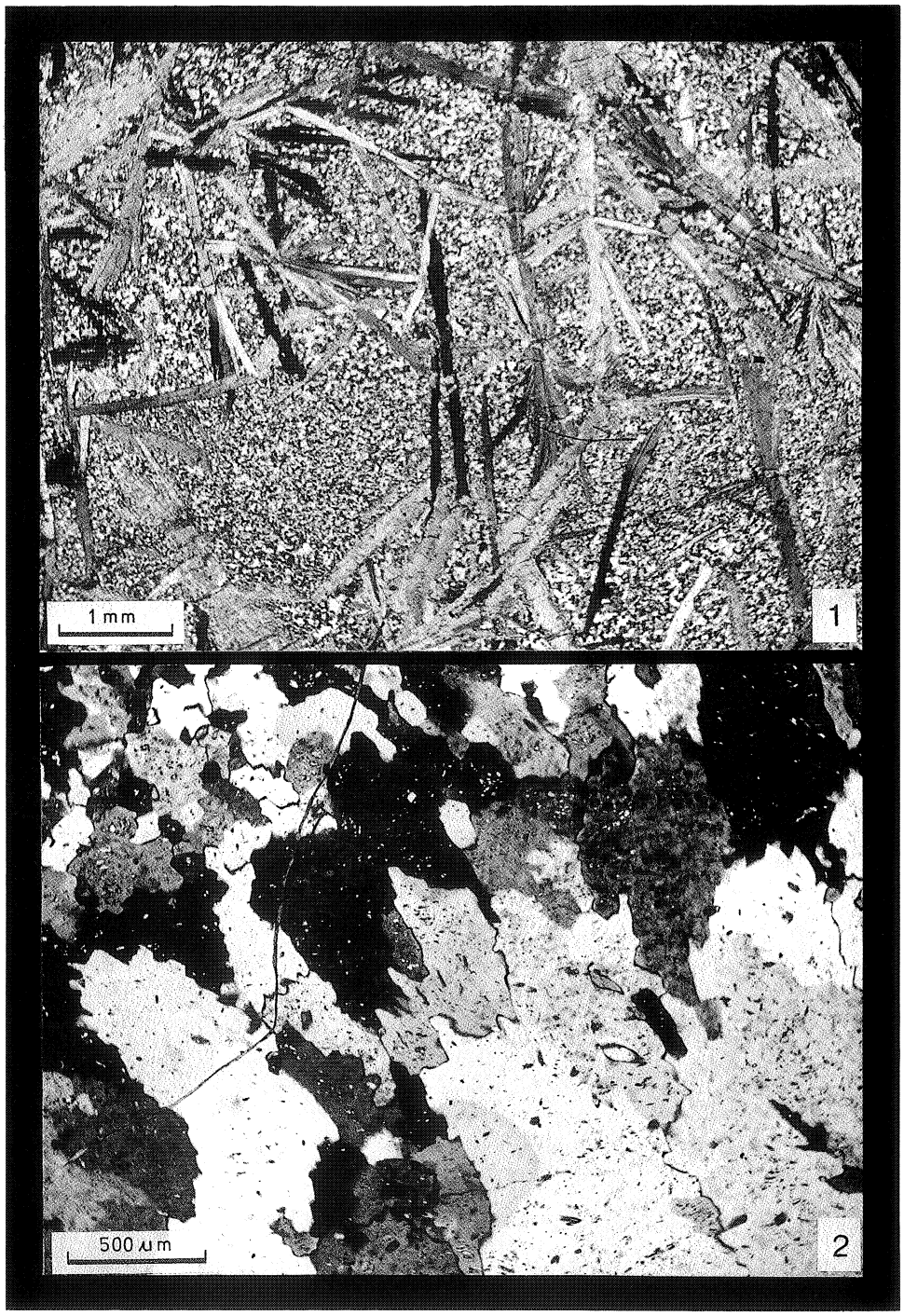
1 mm
1
500 µm
2